Electronic Supplementary Material (ESI) for ChemComm.

Direct Synthesis of Polyureas from the Dehydrogenative Coupling of Diamines and Methanol

Amit Kumar,*† Daniel Armstrong,† Gavin Peters,† Manjula Nagala,‡ Sally Shirran‡

†School of Chemistry, ‡BSRC Mass Spectrometry and Proteomics Facility, University of St. Andrews, North Haugh, St. Andrews, KY169ST, UK.

Table of contents

1. General information

All experiments were carried out under an inert atmosphere of purified nitrogen using standard Schlenk techniques unless specified. Diamines, anhydrous methanol, and complexes **1**-**6** were purchased from Sigma- Aldrich, Alfa Aesar, Strem, or TCI and used as received. THF and toluene were dried using a solvent purification system and degassed by Freeze-Pump-Thaw under nitrogen. Anhydrous anisole and DMSO were purchased from Sigma-Aldrich and used as received. $^{13}CH_3OH$ was purchased from Sigma-Aldrich and degassed by bubbling nitrogen gas before use. Deuterated solvents – $CDCl_3$ and CF_3COOD were purchased from Sigma-Aldrich and used as received.

For the preparation of the MALDI samples, polyureas were dissolved in neat TFA and further diluted with 0.1% TFA (prepared in HPLC grade water). 0.5 µL of the resulting solution was applied to a stainless steel MALDI target plate, 0.5 µL of the matrix was co-spotted and allowed to dry. Matrix was either 2,5-dihydroxybenzoic acid or alpha-cyano-4-hydroxycinnamic acid prepared at 10 mg/mL in 50:50 acetonitrile: 0.1% TFA. MALDI data was acquired using a 4800 MALDI TOF/TOF Analyser (Sciex) equipped with a Nd:YAG 355 nm laser. The sample was acquired in positive MS mode between 200 m/z and 4000 m/z in reflector mode or 3000m/z-10000m/z in linear mode. The instrument was externally calibrated in reflector mode using Sciex 6 peptide TOF/TOF calibration mix, and in linear mode with ubiquitin protein.

^{1}H and $^{13}C\{1H\}$ NMR experiments were carried out at 298 K using Bruker Avance III 500 (500 MHz ^{1}H, 125 MHz ^{13}C) and reported in ppm (δ). NMR spectroscopy abbreviations: br, broad; s, singlet; d, doublet; t, triplet; m, multiplet.

GC was carried out on the instrument from Agilent Technologies equipped with five valves and three detectors. The FID channel (first detector) is configured to analyse hydrocarbons. The first TCD channel (second detector, reference gas He) is configured to analyse N_2, CO_2, CO, and O_2. The second TCD channel (third detector) is dedicated to analyse H_2 gas only.

IR spectra were recorded using a MIRacle^{TM} single reflection horizontal ATR accessory from Pike (ZnSe single crystal) to analyse a neat solid sample of polyureas.

Thermal gravimetric analysis (TGA) was carried out using a Stanton Redcroft STA780 with a heating rate of 10 °C/min from 50 to 500 °C in an N_2 flow. Decomposition temperatures (T_d) were recorded by the thermal gravimetric analysis (TGA) at the 5% weight loss. Differential Scanning Calorimetry (DSC) of the polyureas were measured on a Netzsch DSC204F1 with a heating and cooling rate of 10 °C/min between -100 and 400 °C in an N_2 atmosphere. The first cycle was run from 25 °C to -100 °C and then -100 °C to

250 °C. The second cycle was run from 250 °C to -100 °C and then -100 °C to 400 °C. All T_m, and T_g measurements were taken from the second cooling/heating segments. In some cases, a small hump/band is obtained in the first cycle at temperature below 120 °C which is attributed to the loss of residual solvent or diamines. Values of the decomposition temperature (T_d) from TGA are in agreement with those from the DSC measurements.

Optical rotation measurements were taken on a Perkin Elmer 341 polarimeter using a 1 mL cell with a 1 dm path length at 20 °C using the sodium D-line. The sample was prepared by dissolving polyurea or diamine in TFA with a concentration of 10 mg/mL.

2. General procedure for the synthesis of polyureas

Ruthenium complex (0.02 mmol), KO^{t}Bu (0.04 mmol), and diamine (2 mmol) were weighed (under air) in a Young's flask (volume 100 mL) containing a stirrer bar and then degassed using three vacuum/nitrogen cycles in a Schlenk line. A solvent was added (2 mL) to it followed by the addition of methanol (3.2 mL, 8 mmol) both under nitrogen. The resulting reaction mixture was refluxed by placing Young's flask in an oil bath at 130 °C. After completion of the reaction time, the reaction mixture was cooled to room temperature. In the cases of polyureas corresponding to the Table 2 entries 3-10 (see manuscript), the formation of an off-white precipitate was obtained whereas in the cases of the entries 1-2, Table 2 (see manuscript) no precipitate was obtained but rather an oily layer separated out from the reaction mixture. The product was isolated as specified below. The obtained products were analyzed by NMR and IR spectroscopy, MALDI-TOF mass spectrometry, and TGA-DSC studies.

Note: Caution must be taken as the reaction can produce up to ~160 mL of H_2 gas (298 K) in a sealed flask.

Isolation of products for the entries 3-10, Table 2

A light yellow-white precipitate was obtained after the completion of the reaction time. The reaction flask was cooled to room temperature. The precipitate was filtered off and washed with $CHCl_3$, toluene, and pentane. The obtained solid was dried under vacuum.

Isolation of products for the entries 1-2, Table 2

No precipitate was obtained after the completion of the reaction time. The reaction flask was cooled to room temperature which resulted in the formation of an oily layer. The reaction mixture was kept in a freezer at -30 °C for 30 minutes which resulted in the formation of a white precipitate. The solution was decanted off and the precipitate was washed off with pentane, toluene (and $CHCl_3$ in case of entry 2) and

dried under vacuum. It is noteworthy that the polyurea corresponding to Table 1 entry 1 is soluble in $CHCl_3$ which should be avoided for washing.

Procedure for a typical example: Synthesis of polyurea from 4,7,10-Trioxa-1,13-tridecanediamine and methanol (Table 2 entry 1)

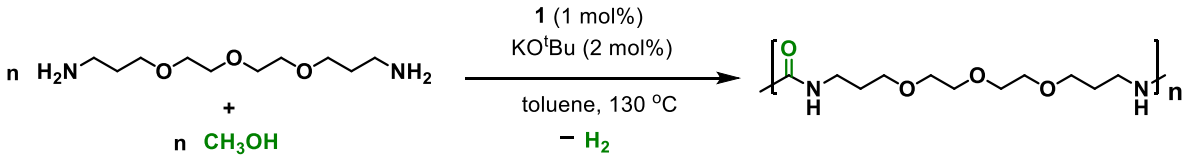

Ruthenium complex (12 mg, 0.02 mmol), KO^tBu (4.5 mg, 0.04 mmol), and 4,7,10-Trioxa-1,13-tridecanediamine (440 mg, 2 mmol) were weighed (under air) in Young's flask containing a stirrer bar and then degassed using three vacuum/nitrogen cycles in a Schlenk line. Toluene was added (2 mL) to it followed by the addition of methanol (3.2 mL, 8 mmol) both under nitrogen. The resulting reaction mixture was refluxed by placing Young's flask in an oil bath at 130 °C. After completion of the reaction time, the reaction mixture was cooled to room temperature. The formation of a precipitate was not observed but rather an oily layer separated out from the reaction mixture. The reaction mixture was kept in a freezer at -30 °C for 30 minutes which resulted in the formation of a white precipitate. The solution was decanted off and the precipitate was washed off with pentane and toluene and dried under vacuum. The obtained product was analyzed by NMR and IR spectroscopy, MALDI-TOF mass spectrometry, and TGA-DSC studies.

Procedure for a typical example: Synthesis of polyurea from diaminohexane and methanol (Table 2, entry 3)

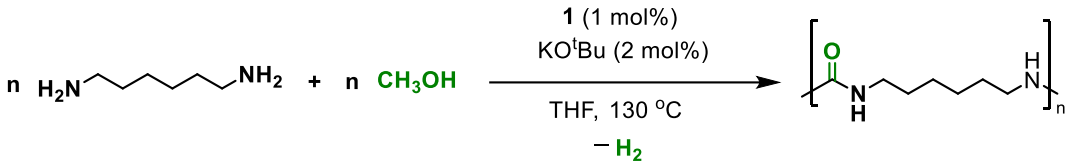

Ruthenium complex (12 mg, 0.02 mmol), KO^tBu (4.5 mg, 0.04 mmol), and diaminohexane (232 mg, 2 mmol) were weighed (under air) in Young's flask containing a stirrer bar and then degassed using three vacuum/nitrogen cycles in a Schlenk line. THF was added (2 mL) to it followed by the addition of methanol (3.2 mL, 8 mmol) both under nitrogen. The resulting reaction mixture was refluxed by placing Young's flask in an oil bath at 130 °C. After completion of the reaction time, the reaction mixture was cooled to room temperature. Formation of an off-white precipitate was formed at the end of the reaction time. The

precipitate was filtered off and washed with $CHCl_3$, toluene, and pentane and dried in vacuum. The obtained products were analyzed by NMR and IR spectroscopy, mass spectrometry, and TGA-DSC studies.

3. Solubility of polyureas

The solubility of polyureas (Table 2, entries 1-10) were tested by adding 10 mg of a polyurea in a vial containing 2 mL of a solvent ($CHCl_3$, THF, acetone, H_2O, DMF, DMSO, TFA). Polyurea corresponding to entry 1, Table 2 was found to dissolve in $CHCl_3$, H_2O, acetone, DMF, DMSO, and TFA. Other polyureas (Table 2, entries 2-10) were found to be insoluble under these conditions in $CHCl_3$, THF, H_2O, DMF, DMSO, TFA. All of them exhibited some solubility in TFA.

4. Detection of gas using GC

A reaction was carried in Young's flask as described above in Section 2. Young's flask was cooled to room temperature after completion of the reaction time. The side outlet was evacuated using a suba-seal and a needle that was connected to the Schlenk line. The tap of Young's flask was opened slightly while a 100 mL syringe was connected to the suba-seal through a needle. This automatically filled the syringe with the gas pressure present in Young's flask. The syringe was injected into the GC to detect gases present. Gas chromatogram showed H_2 gas to be the major constituent whereas CO_2 and CO were also detected in small quantities. We speculate that CO_2 is produced from the aqueous reforming of methanol due to traces of water present in the system.[1] CO could result from the decarbonylation of formaldehyde.[2]

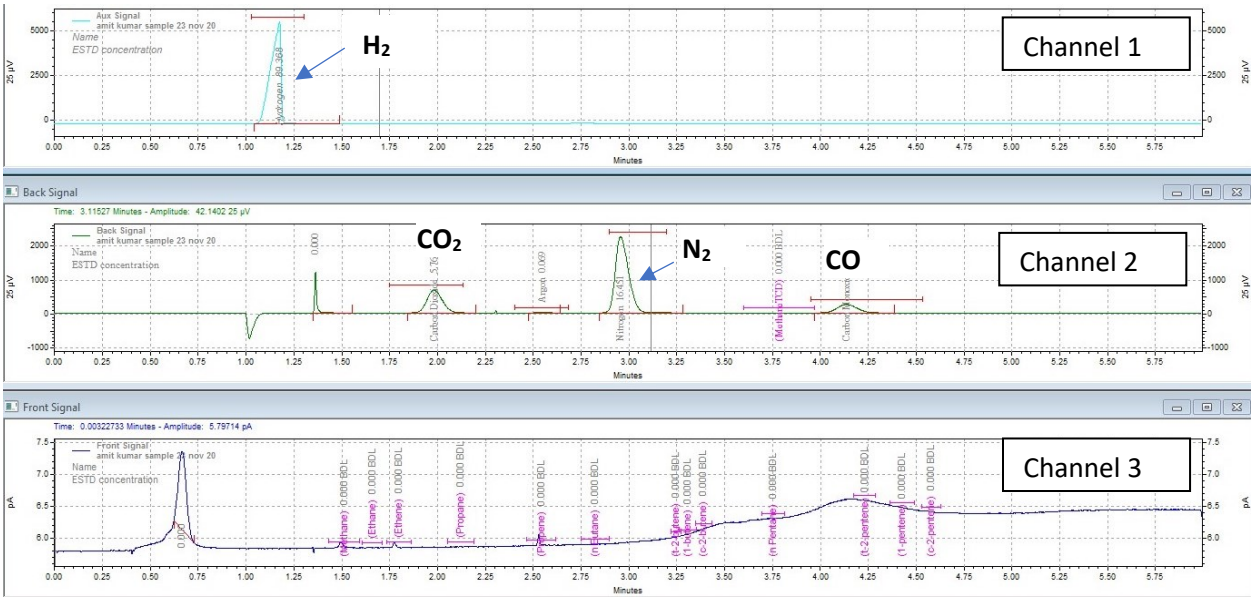

Figure S1. Gas chromatogram measured for the gases present in the Young's flask.

5. Correlation of reaction time with polymer chain length

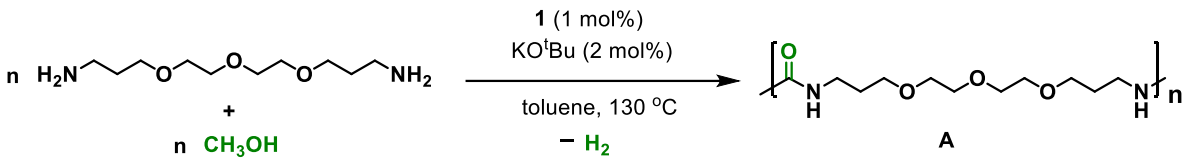

Experiments were conducted to study the correlation between reaction time and polymer chain length. Catalytic dehydrogenative coupling reactions between 4,7,10-Trioxa-1,13-tridecanediamine and methanol were conducted using the method described in Section 2 at a reaction time of 6 h, 12 h, 24 h, and 48 h. The results are summarized in Table S1. The results showed that the polymer chain length increases on increasing reaction time from 6 h to 24 h. However, not much increment is observed during 24 h-48 h. This could be due to the insolubility of longer polymer chains or catalyst decomposition.

Table S1. Molecular weight (M_n) of the polyurea **A** at different reaction times.

Entry	Reaction time	M_n
1.	6 h	950
2.	12 h	2200
3.	24 h	4060
4.	48 h	4300

6. Determination of molecular weight of polyureas using ^{1}H NMR spectroscopy

The molecular weight (M_n) of polyureas was determined by the end group analysis using the ^{1}H NMR spectroscopy. The MALDI-TOF mass spectrometry (e.g. see Figure S42) indicated that end groups contain both either an NH_2 group (e.g. PU1) or an NH-CHO group (e.g. PU2). Therefore, the C*H*$_2$ protons next to the NH_2 and NH-CHO groups both were considered as end group for the calculation of M_n. This was compared relative to the protons present in the repeating units depending on the structure of a polyurea. An example has been described here for demonstration. Protons at position *f* (PU1, δ2.87), and position *g* (PU2, δ3.41) were used for the end group. Their combined sum of integration results in a value of 1.28. For the repeating unit, the protons at position *d* (PU1, PU2, δ1.76-1.82) were used whose integration value is 24.54. In any polymer chain analysed in this report, there will be 2 CH_xN- end groups (x = 1-2, in this case x =2), one on each side whether the end group is NH_2 or NHCHO. In this case, the repeating unit

also has 2 CH_2 protons corresponding to position *d*. Therefore, the number of repeating units can be calculated by:

$$\text{No of repeating units} = \frac{\text{integration of protons at position } d}{\text{integration of protons at position } f + \text{integration of protons at position } g} = \frac{24.54}{1.28} = 19.17$$

M_n is calculated by multiplying the formula weight of the repeating unit (248.17) with the number of repeating units (19.17) resulting in 4757. For simplicity, the addition of the formula weight of the end group to 4757 is not carried due to the possibility of two end groups. It is noteworthy that the M_n calculated using this method is just an estimate and can deviate from the accurate values due to: (a) the possibility of precision error while integrating the NMR signals, and (b) poor solubility of polyureas (in some cases) in the deuterated solvents used for the NMR studies.

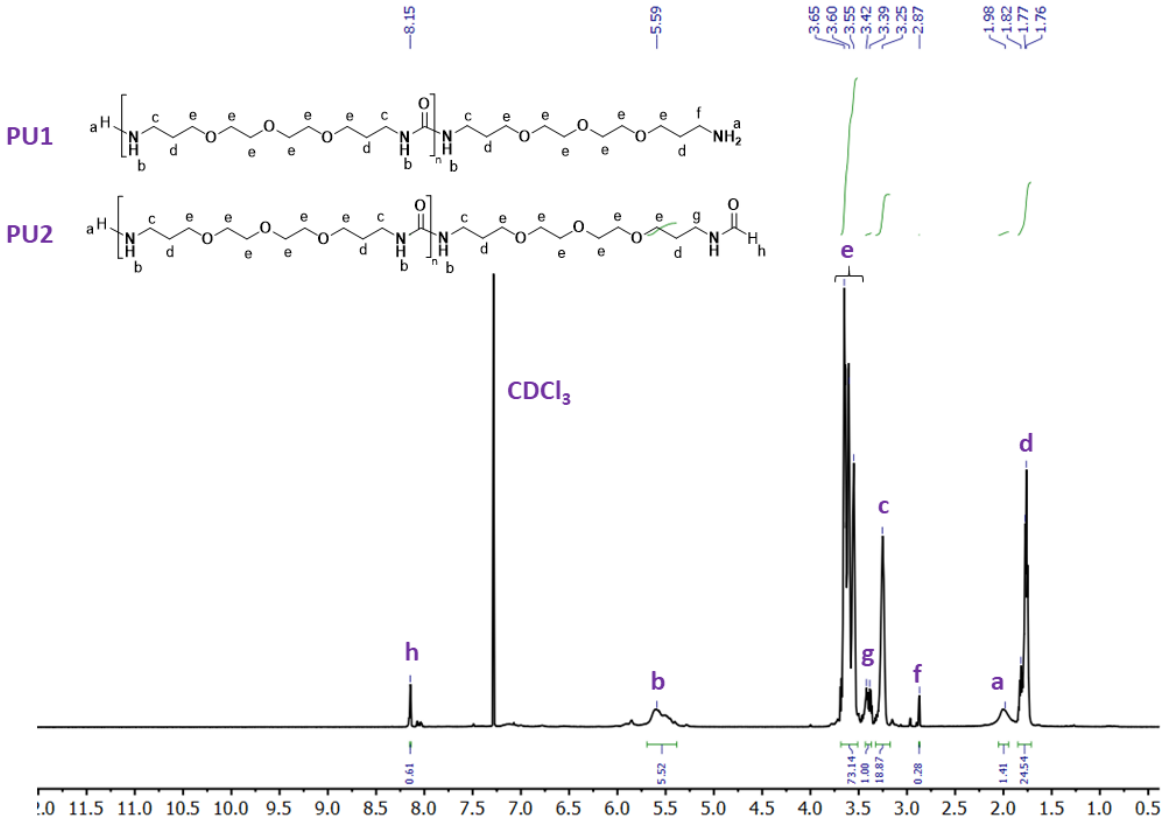

Figure S2. ^{1}H NMR spectrum ($CDCl_3$, 500 MHz, 298 K) of the polyurea of the depicted structure.

7. Characterisation data of the isolated polyurea

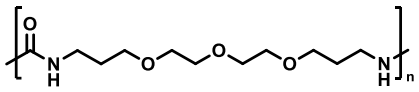

^{1}H NMR (500 MHz, $CDCl_3$, 298 K): δ 1.76-1.82 (m, 24 H), 1.98 (br, 1 H), 2.87 (s, 0.28 H), 3.25 (br, 19 H), 3.41 (m, 1 H), 3.55-3.65 (m, 73 H), 5.59 (br, 6 H), 8.15 (s, 0.61 H).

^{13}C{^{1}H} NMR (125 MHz, $CDCl_3$, 298 K): δ 27.6, 28.5, 30.1, 36.4, 37.8, 41.1, 69.4, 69.5, 70.0, 159.2, 161.8.

IR (ATR, cm^{-1}): 3319, 2933, 2856, 1612, 1570.

MALDI-TOF (m/z): 807.4 [M + K^+, (n = 3)], 1053.6 [M + K^+, (n = 4)], 1299.7 [M + K^+, (n = 5)], 1545.9 [M + K^+, (n = 6)], 1792.0 [M + K^+, (n = 7)], 2038.2 [M + K^+, (n = 8)], 2284.3 [M + K^+, (n = 9)], 2530.5 [M + K^+, (n = 10)], 2776.6 [M + K^+, (n = 11)], 3022.8 [M + K^+, (n = 12)].

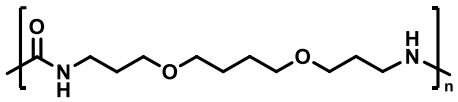

^{1}H NMR (500 MHz, CF_3COOD, 298 K): δ 2.27 (br, 24 H), 2.54 (br, 24 H), 3.99 (br, 23 H), 4.16 (br, 1H), 4.24-4.30 (br m, 46 H), 5.36 (s, 1H), 5.36 (s, 1H), 8.68 (br, 1H), 8.94 (br, 1H).

^{13}C{^{1}H} NMR (125 MHz, CF_3COOD, 298 K): δ 24.1, 26.4, 26.9, 37.1, 37.9, 67.0, 67.4, 70.4, 159.2, 165.2, 167.7.

IR (ATR, cm^{-1}): 3323, 2935, 2858, 1612, 1587, 1112.

MALDI-TOF (m/z): 463.5 [M + H^+, (n = 2)], 491.5 [M + H^+, (n = 2')], 693.8 [M + H^+, (n = 3)], 721.8 [M + H^+, (n = 3')], 923.9 [M + H^+, (n = 4)], 951.9 [M + H^+, (n = 4')].

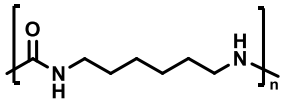

^{1}H NMR (500 MHz, d-TFA, 298 K): δ 1.74 (br, 27 H), 2.0 (br, 26 H), 2.14 (br, 0.56 H), 3.25 (br, 0.67 H), 3.66 (br, 25 H), 3.92 (br, 2 H), 7.28 (br, 1 H), 8.79 (br, 1 H).

^{13}C{^{1}H} NMR (125 MHz, CF_3COOD, 298 K): δ 26.5, 29.0, 34.5, 42.6, 159.8, 166.2.

IR (ATR, cm^{-1}): 3329, 2933, 2854, 1612, 1577.

MALDI-TOF (m/z): 543.5 [M + H^+, (n = 4)], 685.6 [M + H^+, (n = 5)], 827.7 [M + H^+, (n = 6)], 969.8 [M + H^+, (n = 7)], 1112.0 [M + H^+, (n = 8)], 1254.1 [M + H^+, (n = 9)], 1396.2 [M + H^+, (n = 10)], 1538.3 [M + H^+, (n = 11)].

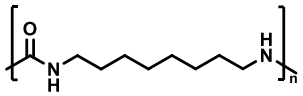

^{1}H NMR (500 MHz, CF_3COOD, 298 K): δ 1.75 (br, 50 H), 2.04 (br, 23 H), 2.17 (br, 0.38 H), 3.61 (br, 0.57 H), 3.72 (br m, 22 H), 3.96 (t, 1H), 8.56 (br, 1 H), 8.87 (br, 1 H).

$^{13}C\{^1H\}$ NMR (125 MHz, CF_3COOD, 298 K): δ 26.1, 28.6, 42.0, 158.9.

IR (ATR, cm^{-1}): 3334, 2927, 2852, 1612, 1568.

MALDI-TOF (m/z): 875.6 [M + Na^+, (n = 5)], 1045.8 [M + Na^+, (n = 6)], 1216.6 [M + Na^+, (n = 7)], 1401.0 [M + K^+, (n = 8)], 1571.1 [M + K^+, (n = 9)].

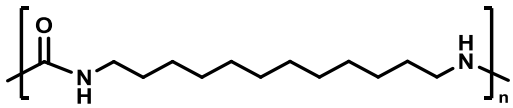

^{1}H NMR (500 MHz, CF_3COOD, 298 K): δ 1.87-1.91 (br m, 70 H), 2.20 (br, 16 H), 2.57 (br, 1 H), 3.88 (br, 1 H), 4.14 (br, 1H), 4.42 (br, 1 H), 4.51 (br, 1 H), 8.73 (s, 1H), 9.04 (s, 1H).

$^{13}C\{^1H\}$ NMR (125 MHz, CF_3COOD, 298 K): δ 25.6, 27.0, 27.8, 28.0, 28.1, 28.5, 41.0, 41.4, 158.2, 164.7.

IR (ATR, cm^{-1}): 3338, 2920, 2848, 1610, 1573.

MALDI-TOF (m/z): 747.6 [M + K^+, (n = 3)], 973.8 [M + K^+, (n = 4)], 1200.0 [M + K^+, (n = 5)], 1426.2 [M + K^+, (n = 6)], 1652.4 [M + K^+, (n = 7)], 1878.6 [M + K^+, (n = 8)] .

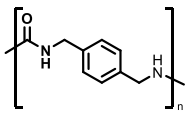

^{1}H NMR (500 MHz, CF_3COOD, 298 K): δ 4.31 (br, 1 H), 4.46 (br, 16 H), 7.23-7.4 (br m, 14 H), 7.45 (br, 1 H), 8.12 (br, 1 H), 8.44 (br, 1 H).

$^{13}C\{^{1}H\}$ NMR (125 MHz, CF_3COOD, 298 K): δ 45.4, 45.7, 45.8, 46.0, 129.1, 129.5, 130.8, 131.9, 136.2, 138.5, 160.4.

IR (ATR, cm^{-1}): 3317, 1614, 1568, 598.

MALDI-TOF (m/z): 689.7 [M + K^+, (n = 4)], 851.8 [M + K^+, (n = 5)], 1014.0 [M + K^+, (n = 6)], 1176.2 [M + K^+, (n = 7)], 1338.4 [M + K^+, (n = 8)], 1500.4 [M + K^+, (n = 9)], 1662.4 [M + K^+, (n = 10)], 1824.9 [M + K^+, (n = 11)].

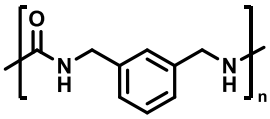

^{1}H NMR (500 MHz, CF_3COOD, 298 K): δ 4.93 (br, 13 H), 5.06 (br, 1 H), 7.50 (br m, 10 H), 7.8 (m, 3H), 8.6 (br, 1 H), 8.9 (br, 1 H).

$^{13}C\{^{1}H\}$ NMR (125 MHz, CF_3COOD, 298 K): δ 45.2, 126.7, 127.7, 130.1, 135.9, 159.5.

IR (ATR, cm^{-1}): 3317, 1612, 1583, 634.

MALDI-TOF (m/z): 1041.3 [M + K^+ (n=6)], 1204.1 [M + K^+ (n=7)], 1366.3, [M + K^+ (n=8)], 1528.3, [M + K^+ (n=9)], 1690.2, [M + K^+ (n=10)], 1852.2, [M + K^+ (n=11)], 2014.4, [M + K^+ (n=12)], 2176.3, [M + K^+ (n=13)], 2338.3, [M + K^+ (n=14)], 2500.1, [M + K^+ (n=15)].

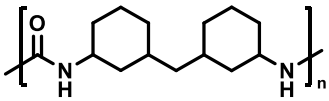

^{1}H NMR (500 MHz, CF_3COOD, 298 K): δ 1.43 (br, 17 H), 1.57-2.30 (br, 160 H), 2.49 (br, 1 H), 3.72 (br, 1 H), 3.94-4.24 (br, 16 H), 7.05 (br, 3 H), 7.63 (s, 2 H), 8.8 (s, 1 H).
$^{13}C\{^{1}H\}$ NMR (125 MHz, CF_3COOD, 298 K): δ 26.6, 27.3, 28.3, 30.6, 31.2, 32.0, 33.3, 52.6, 52.9, 157.2.
IR (ATR, cm^{-1}): 3327, 2920, 2846, 1622, 1556.

MALDI-TOF (m/z): 1013.6 [M + K^+ (n=4)], 1250.2 [M + K^+ (n=5)], 1486.3 [M + K^+ (n=6)], 1722.3 [M + K^+ (n=7)], 1958.7 [M + K^+ (n=8)], 2195.0 [M + K^+ (n=9)], 2431.1 [M + K^+ (n=10)], 2667.3 [M + K^+ (n=11)], 2903.4 [M + K^+ (n=12)], 3139.4 [M + K^+ (n=13)], 3376.1 [M + K^+ (n=14)].

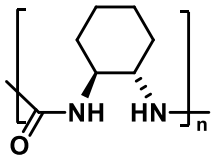

^{1}H NMR (500 MHz, CF_3COOD, 298 K): δ 1.79-2.82 (br m, 173 H), 3.67 (br m, 1 H), 3.99-4.35 (br m, 16 H), 4.48 (br s, 1 H), 7.63 (br, 2 H), 8.68 (br, 1 H), 8.8 (br, 3 H).

$^{13}C\{^{1}H\}$ NMR (125 MHz, CF_3COOD, 298 K): δ 22.8, 23.7, 30.0, 32.0, 54.2, 55.4, 160.0, 165.6.

IR (ATR, cm^{-1}): 3271, 2931, 2854, 1635, 1543.

MALDI-TOF (m/z): 473.3 [M + Na^+ (n=3)], 613.4 [M + Na^+ (n=4)], 753.5, [M + Na^+ (n=5)], 893.6, [M + Na^+ (n=6)], 1033.7, [M + Na^+ (n=7)], 1173.7, [M + Na^+ (n=8)], 1313.8, [M + Na^+ (n=9)].

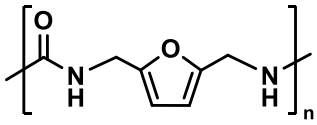

^{1}H NMR (500 MHz, CF_3COOD, 298 K): δ 1.74 (br, 4 H), 2.79 (br, 1 H), 3.07 (br, 1 H), 4.89 (br, 32 H), 7.08 (br, 15 H), 7.87 (br m, 1 H).

$^{13}C\{^{1}H\}$ NMR (125 MHz, CF_3COOD, 298 K): δ 29.5, 37.2, 146.8. Signals from the carbonyl and an aromatic carbon could not be observed due to presumably being obscured by the solvent signal.

IR (ATR, cm^{-1}): 3290, 1651, 1566.

MALDI-TOF (m/z): 307.2 [M + H^+ (n=2', CHO)], 459.8 [M + H^+ (n=3', CHO)], 605.9 [M + Na^+ (n=4)], 758.0 [M + Na^+ (n=5)], 909.5 [M + Na^+ (n=6)].

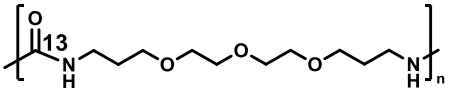

^{1}H NMR (500 MHz, $CDCl_3$, 298 K): δ 1.74-1.81 (br m, 24 H), 3.25 (br, 17 H), 3.42 (br m, 5 H), 3.60-3.64 (br m, 73 H), 7.90 (s, 1 H), 8.38 (s, 1H).

$^{13}C\{^{1}H\}$ NMR (125 MHz, $CDCl_3$, 298 K): δ 28.6, 29.4, 30.0, 34.2, 34.8, 37.8, 51.9, 69.3, 69.8, 70.4, 70.9, 157.3, 158.8, 159.0, 159.2, 161.5, 161.7, 161.9, 164.7, 165.0.

IR (ATR, cm^{-1}): 3321, 2868, 1570.

MALDI-TOF (m/z): 811.7 [M + K^+ (n=3)], 1058.6 [M + K^+ (n=4)], 1305.7 [M + K^+ (n=5)], 1552.8 [M + K^+ (n=6)], 1800.0 [M + K^+ (n=7)], 2047.1 [M + K^+ (n=8)], 2294.3 [M + K^+ (n=9)], 2541.4 [M + K^+ (n=10)], 2788.5 [M + K^+ (n=11)], 3035.7 [M + K^+ (n=12)].

Note: Normally two signals are expected in the carbonyl region of the $^{13}C\{^{1}H\}$ NMR spectra – one due to NH-(**C**=O)-NH group present in the main chain and another one due to NH-(H**C**=O) group from the end chain. In some cases (e.g. Figures S20, S22, S24), the signal corresponding to the end chain formyl group is not observed due to poor solubility of the polyurea. In some cases, such as ^{13}C-labelled polyurea (Figure S30), more than two signals in the carbonyl region are observed. We speculate that other minor signals could be due to the presence of a small amount of (a) smaller oligomer, (b) cyclic urea, or (b) another conformer of the polyurea.[3]

8. Estimation of PDI using MALDI-TOF mass spectrometry

PDI was estimated by calculating M_n and M_w from the MALDI-TOF mass spectrometry data using a method reported in the literature.[4] The M_n values obtained from the MALDI-TOF mass spectrometry method are relatively lower than those obtained using ^{1}H NMR spectroscopy (Table 2 in the manuscript). We speculate that the lower M_n values in the case of the MALDI-TOF mass spectrometry could be because of the relatively poor solubility of polyureas as in the case of the MALDI-TOF mass spectrometry, the sample is diluted with 0.1% TFA (in water) whereas, in case of the ^{1}H NMR spectroscopy, the sample is dissolved in neat TFA. Lower molecular weight values in the case of MALDI-TOF mass spectrometry, in comparison to those obtained from the GPC, have been observed earlier in the case of polyamides.[5]

Table S2. Estimated PDIs of the polyureas using MALDI-TOF mass spectrometry.

Entry	Polymer	M_w	M_n	PDI
1.	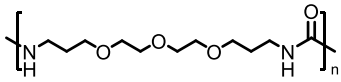	2170	2110	1.03
2.	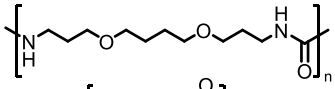	1922	1837	1.04
3.	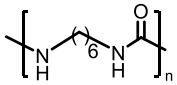	1788	1355	1.32
4.	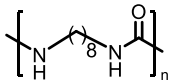	2690	2152	1.25
5.	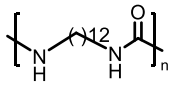	2455	2212	1.11
6.	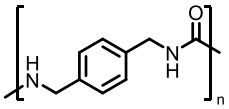	1276	1055	1.21
7.	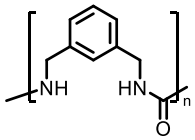	1846	1605	1.15
8.	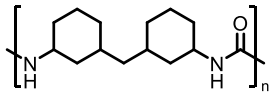	2332	2082	1.12
9.	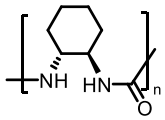	1433	1349	1.06
10.	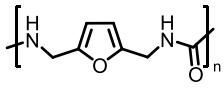	926	850	1.09

9. NMR spectra of the isolated polyureas

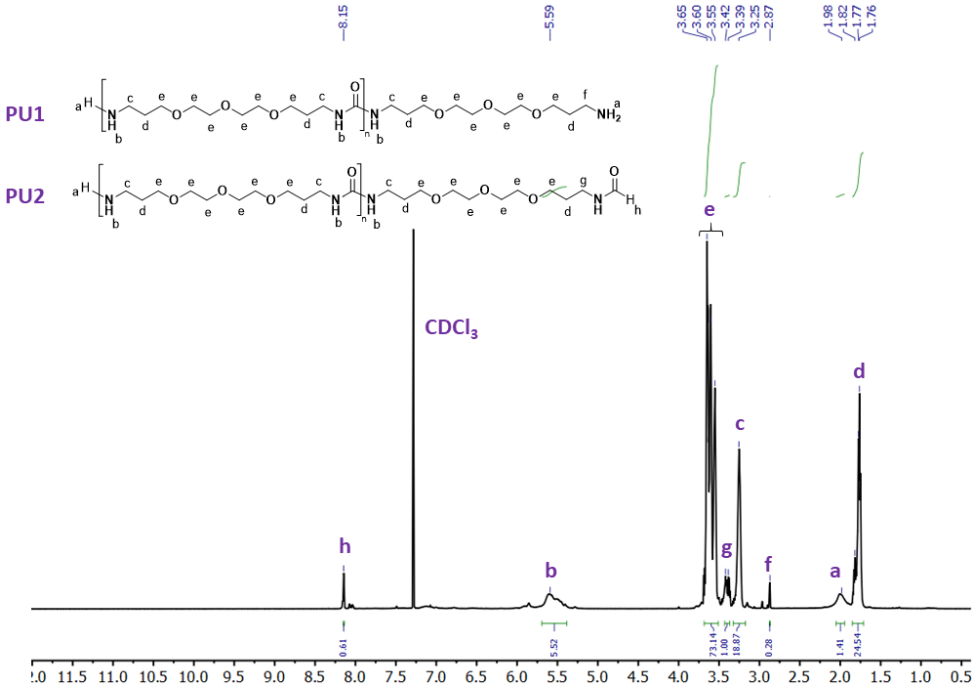

Figure S3. ^{1}H NMR spectrum ($CDCl_3$, 500 MHz, 298 K) of the polyurea of the depicted structure.

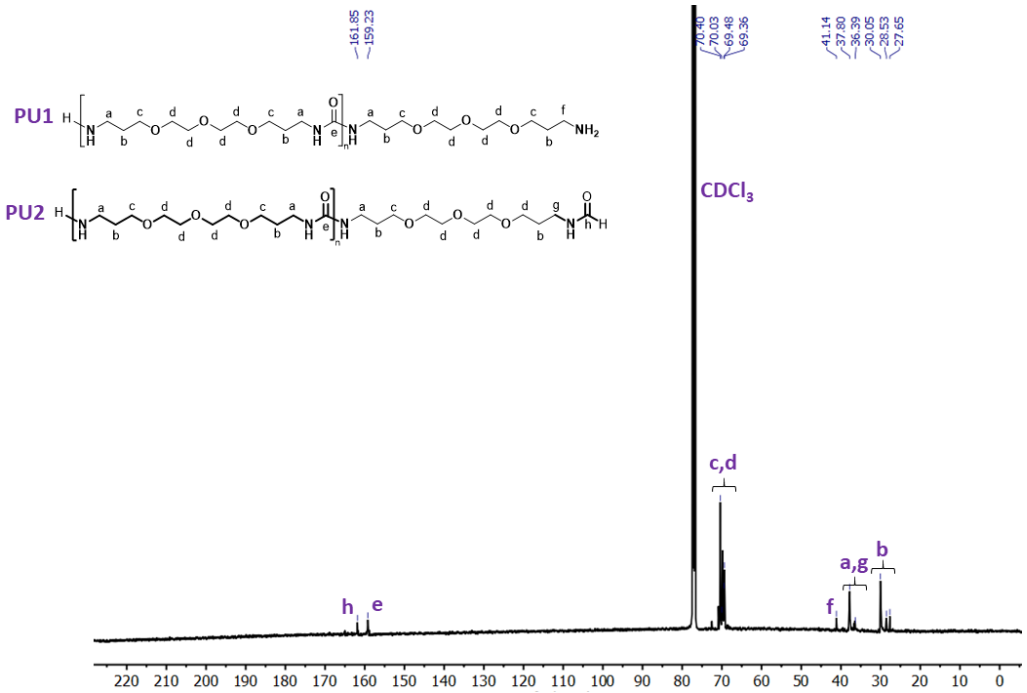

Figure S4. $^{13}C\{^{1}H\}$ NMR spectrum ($CDCl_3$, 125 MHz, 298 K) of the polyurea of the depicted structure.

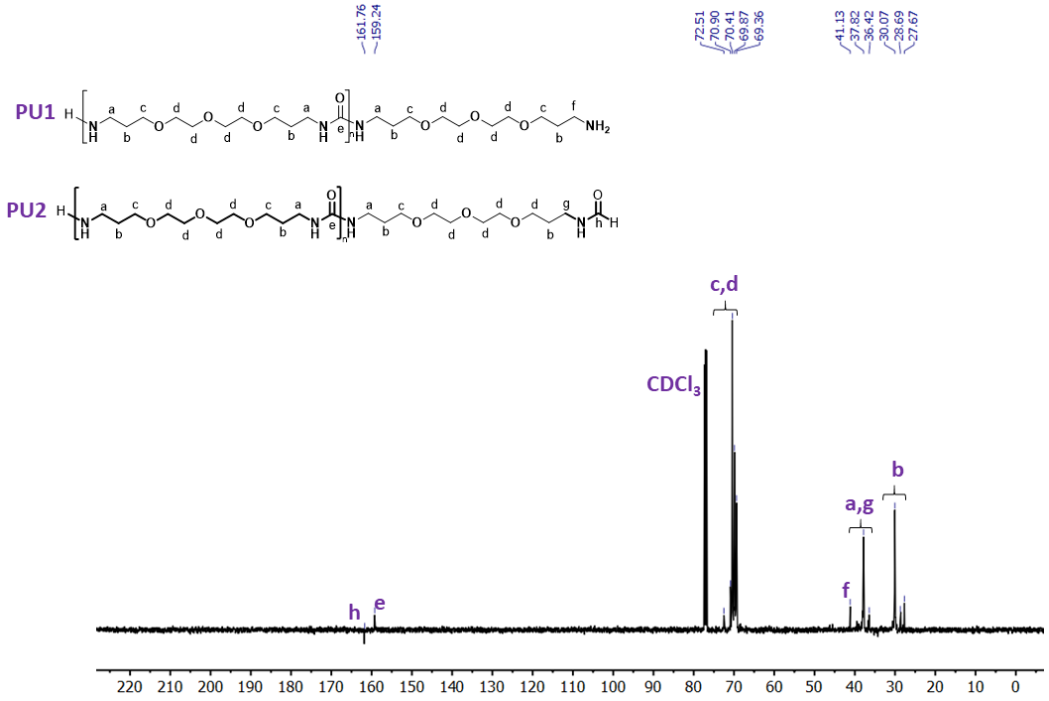

Figure S5. $^{13}C\{^{1}H\}$ DEPTQ NMR spectrum ($CDCl_3$, 125 MHz, 298 K) of the polyurea of the depicted structure.

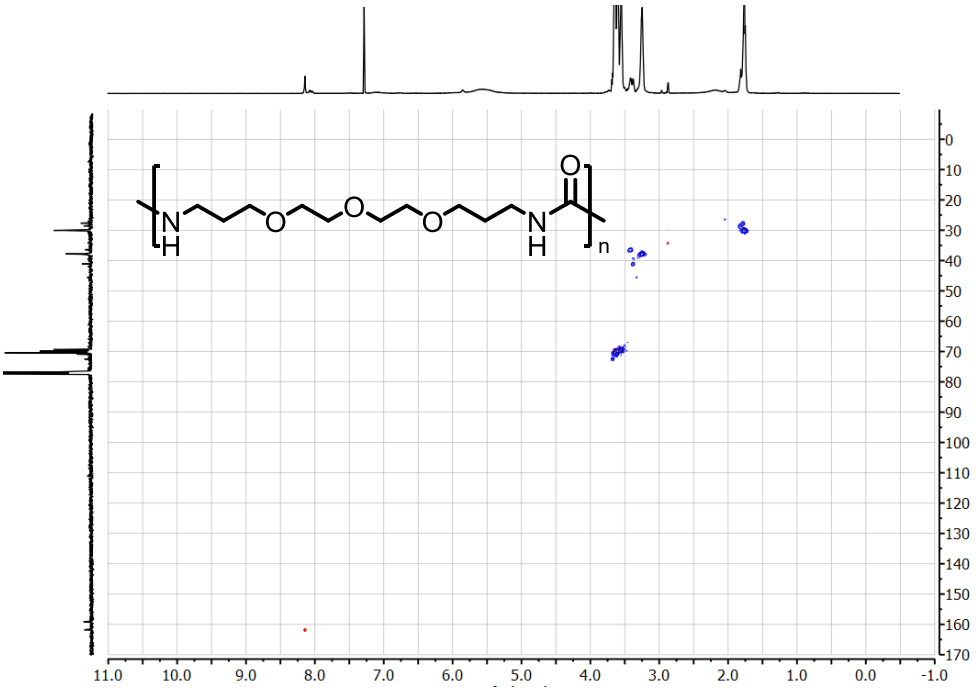

Figure S6. HSQC NMR spectrum ($CDCl_3$, 500 MHz, 298 K) of the polyurea of the depicted structure.

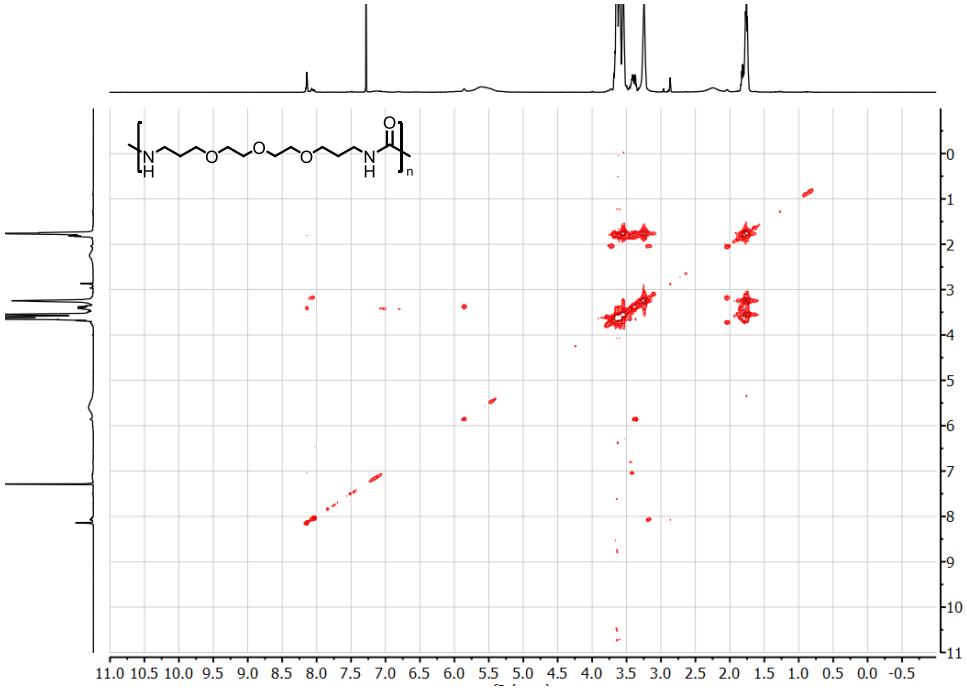

Figure S7. ^{1}H-^{1}H COSY NMR spectrum ($CDCl_3$, 500 MHz, 298 K) of the polyurea of the depicted structure.

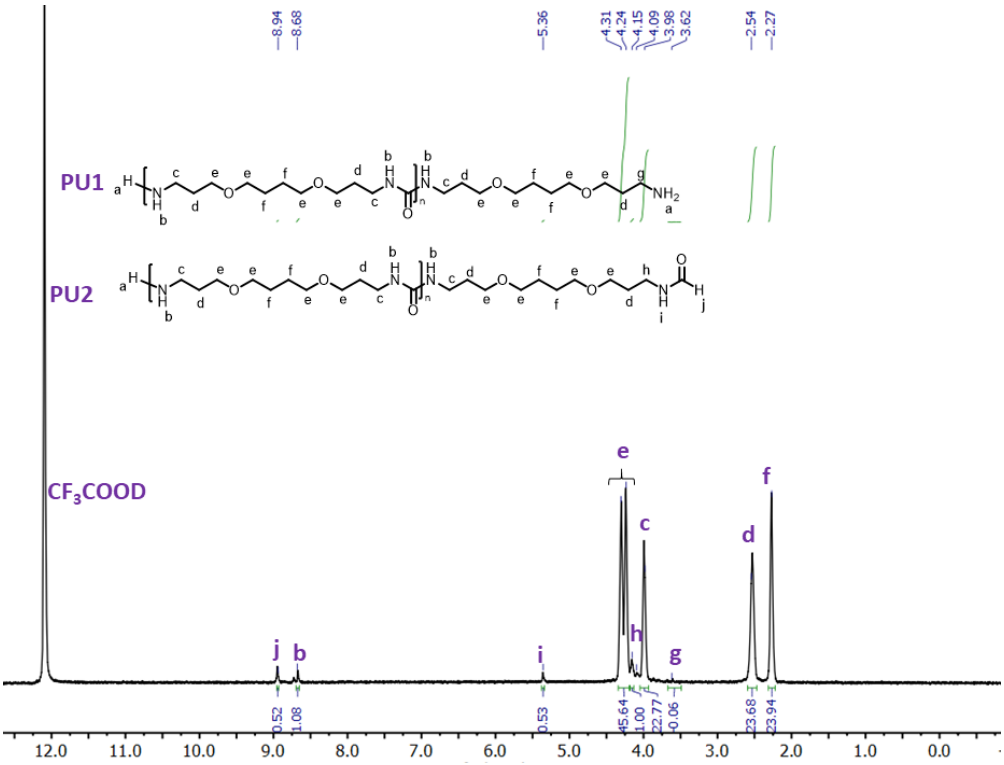

Figure S8. ^{1}H NMR spectrum (CF_3COOD, 500 MHz, 298 K) of the polyurea of the depicted structure.

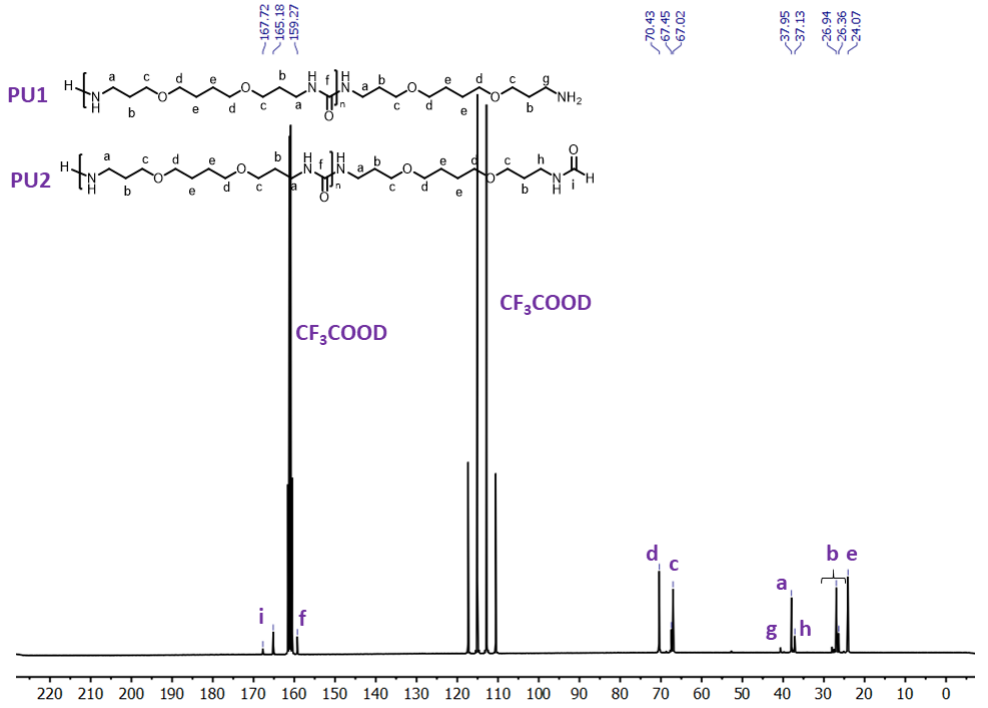

Figure S9. $^{13}C\{^{1}H\}$ NMR spectrum (CF_3COOD, 125 MHz, 298 K) of the polyurea of the depicted structure.

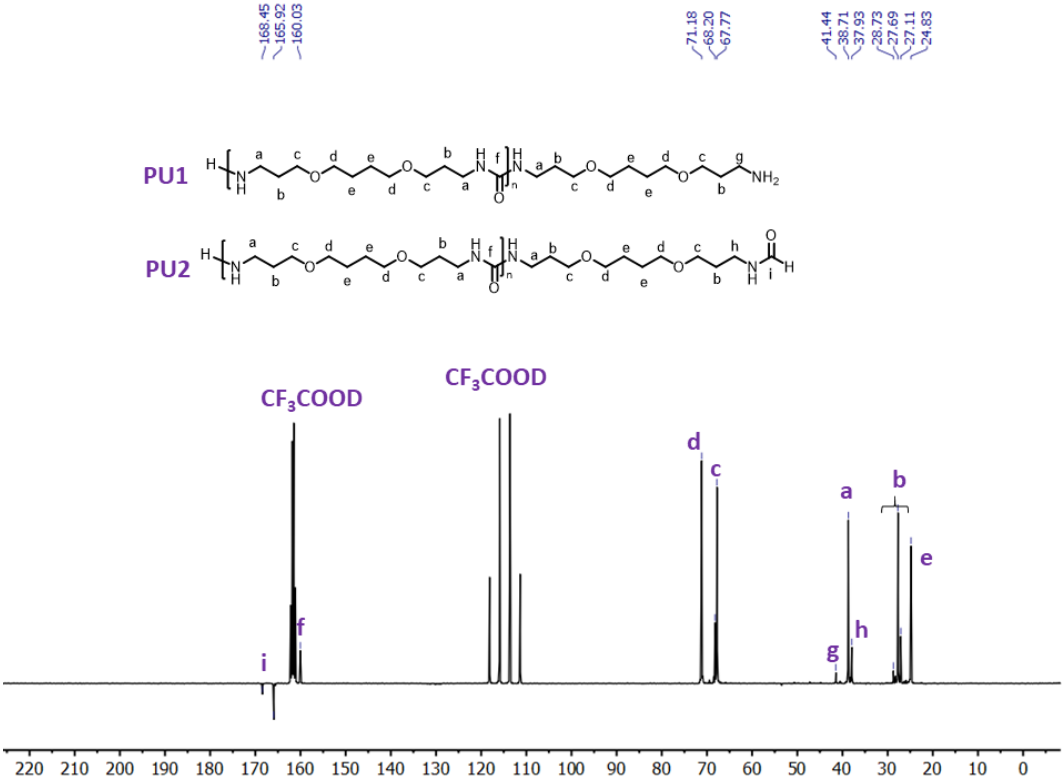

Figure S10. $^{13}C\{^{1}H\}$ DEPTQ NMR spectrum (CF_3COOD, 125 MHz, 298 K) of the polyurea of the depicted structure.

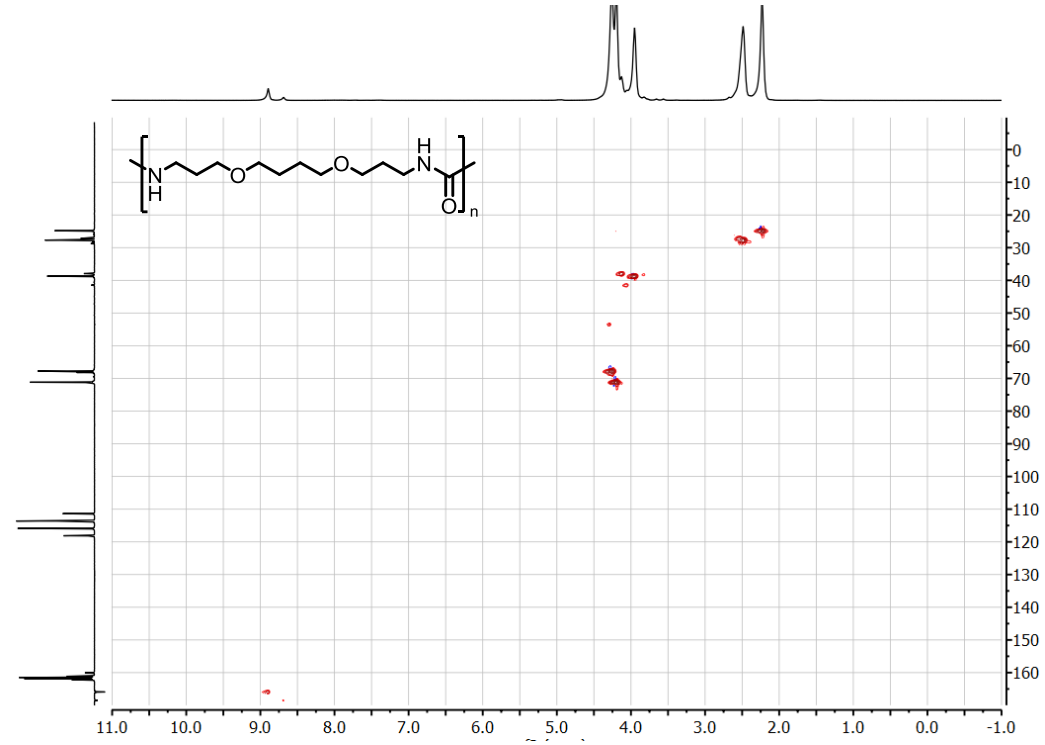

Figure S11. HSQC NMR spectrum (CF_3COOD, 500 MHz, 298 K) of the polyurea of the depicted structure.

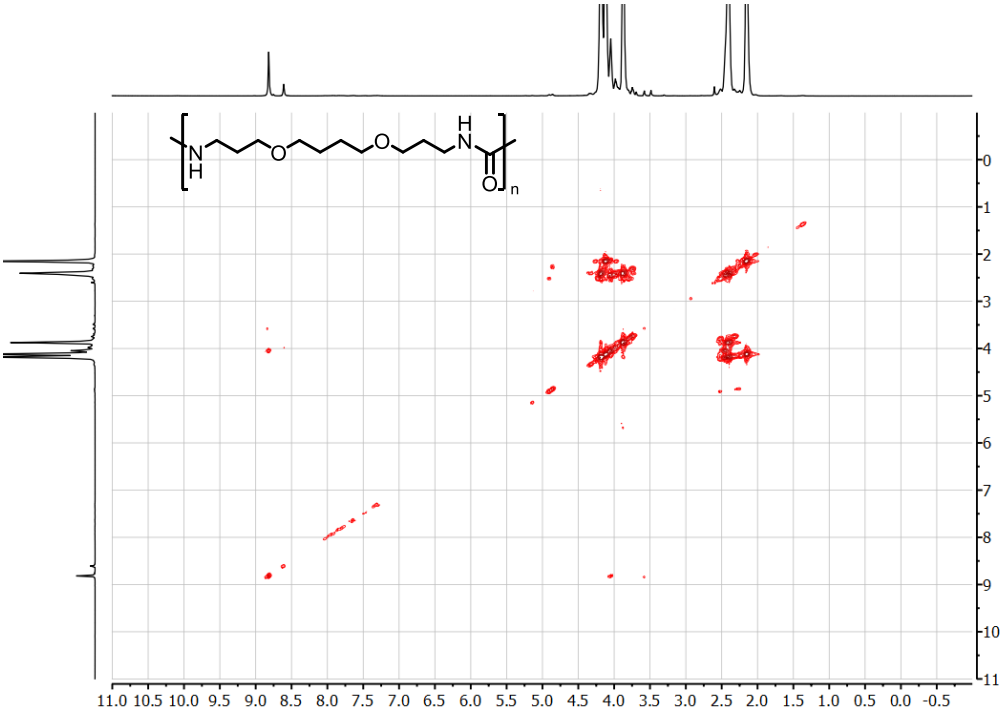

Figure S12. ^1H-^1H COSY NMR spectrum (CF_3COOD, 500 MHz, 298 K) of the polyurea of the depicted structure.

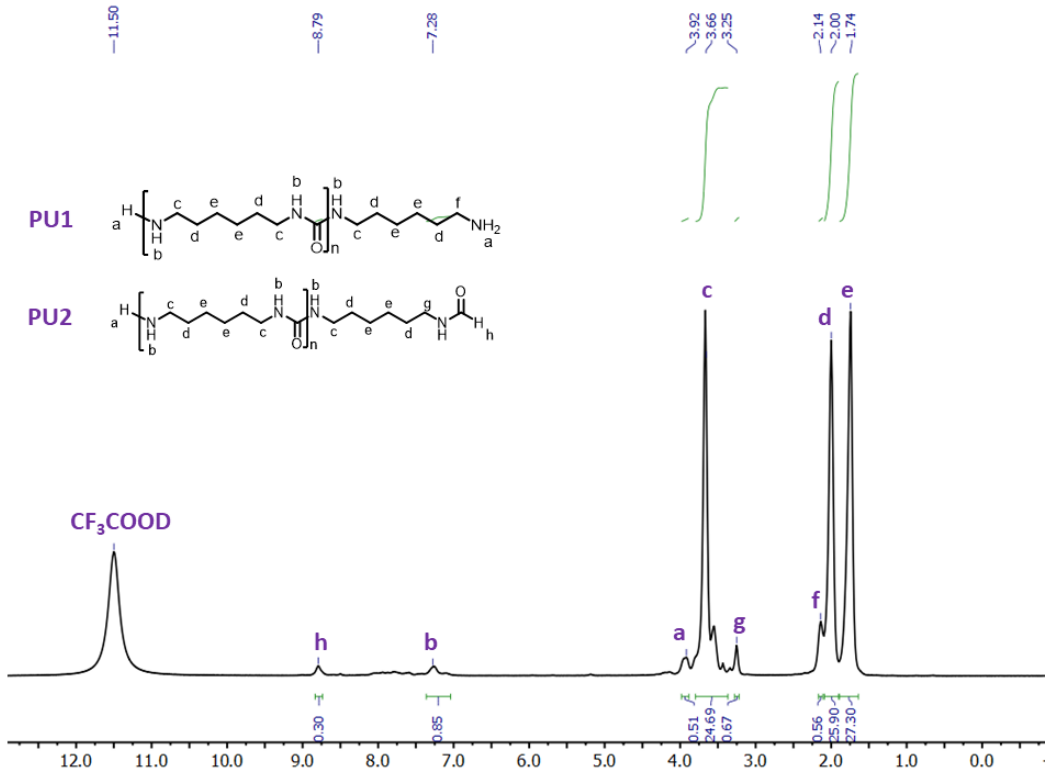

Figure S13. ^{1}H NMR spectrum (CF_3COOD, 500 MHz, 298 K) of the polyurea of the depicted structure.

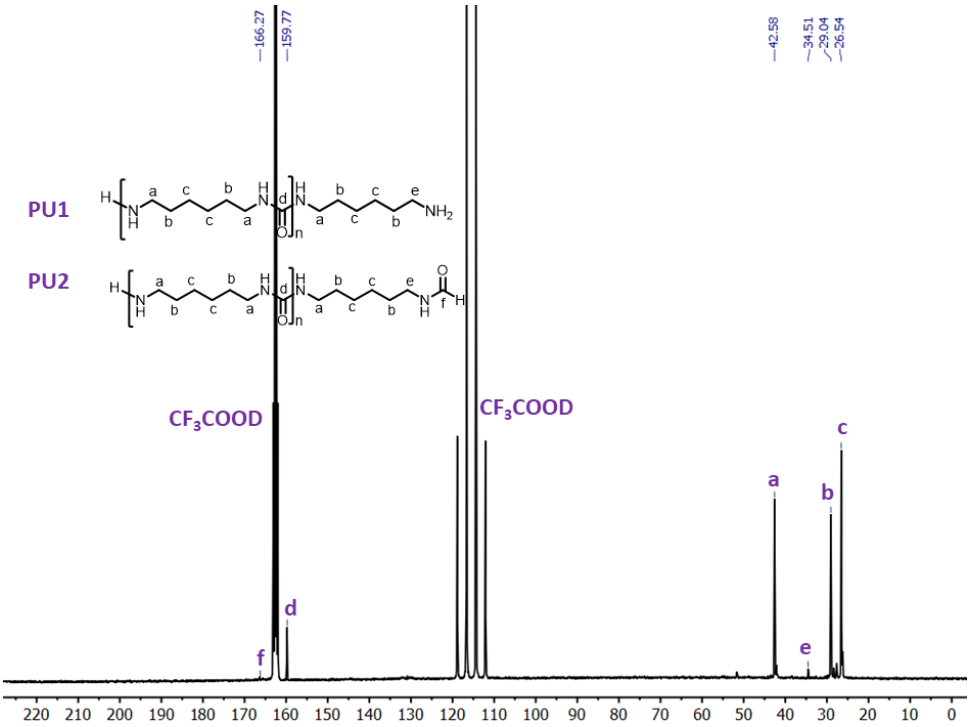

Figure S14. $^{13}C\{^{1}H\}$ NMR spectrum (CF_3COOD, 125 MHz, 298 K) of the polyurea of the depicted structure.

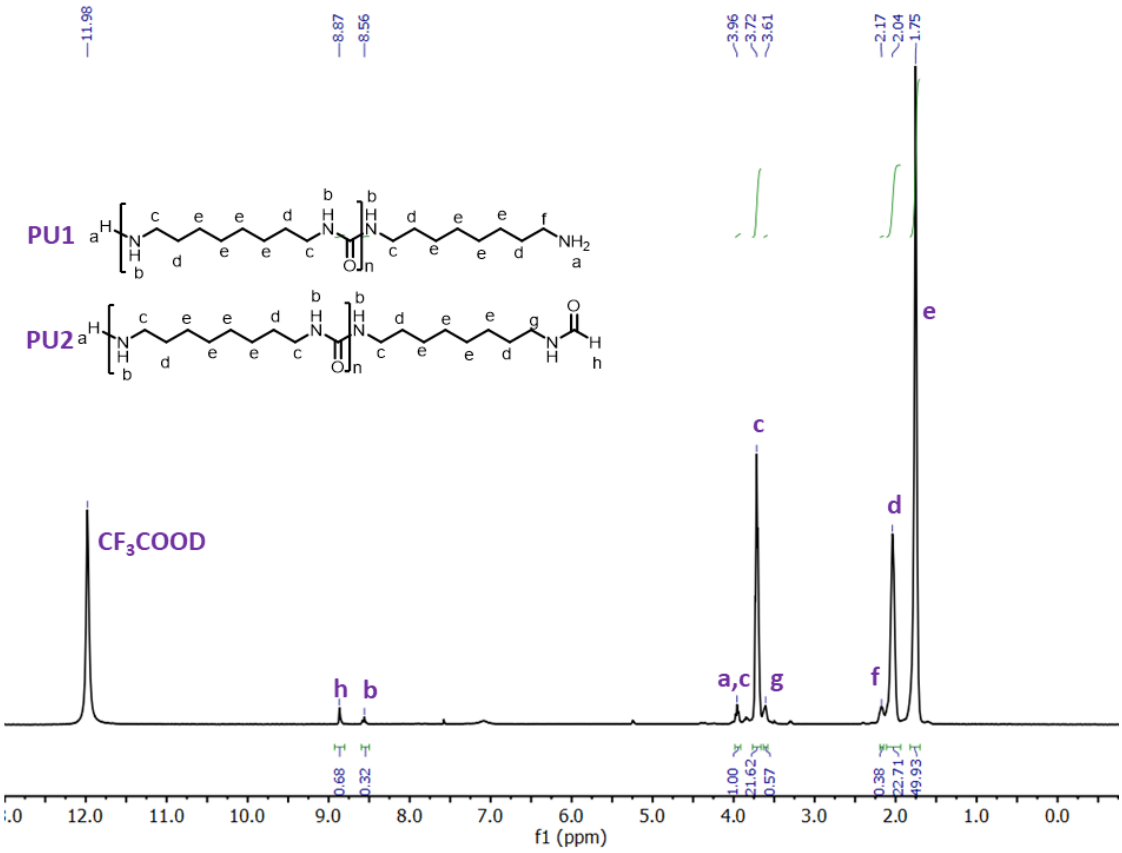

Figure S15. ^{1}H NMR spectrum (CF_3COOD, 500 MHz, 298 K) of the polyurea of the depicted structure.

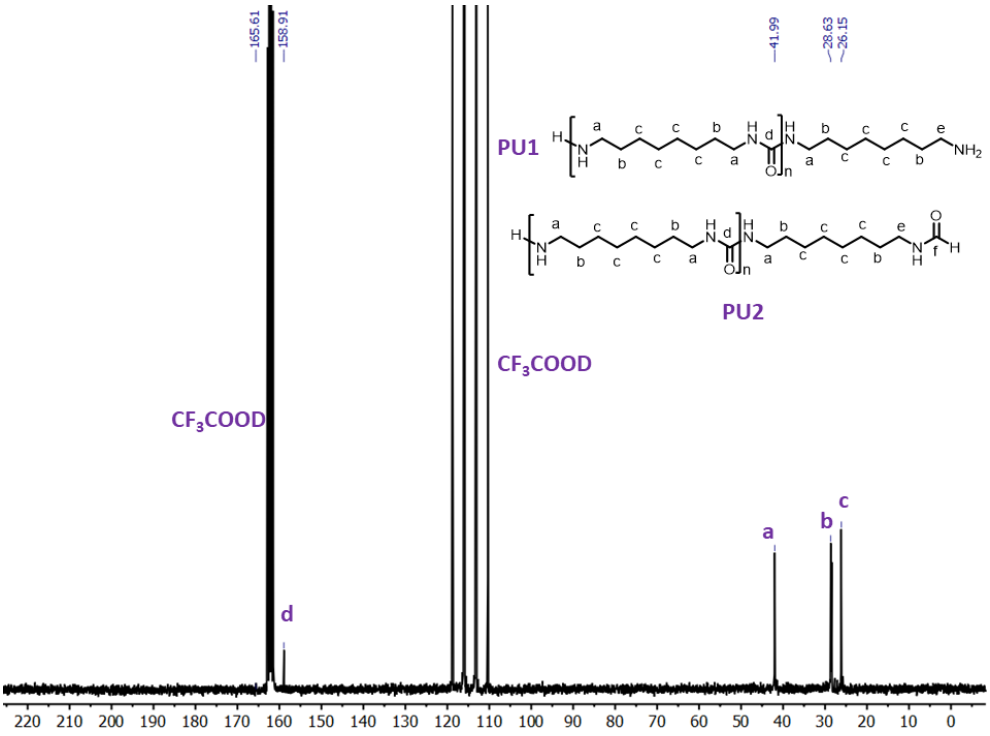

Figure S16. $^{13}C\{^{1}H\}$ NMR spectrum (CF_3COOD, 125 MHz, 298 K) of the polyurea of the depicted structure.

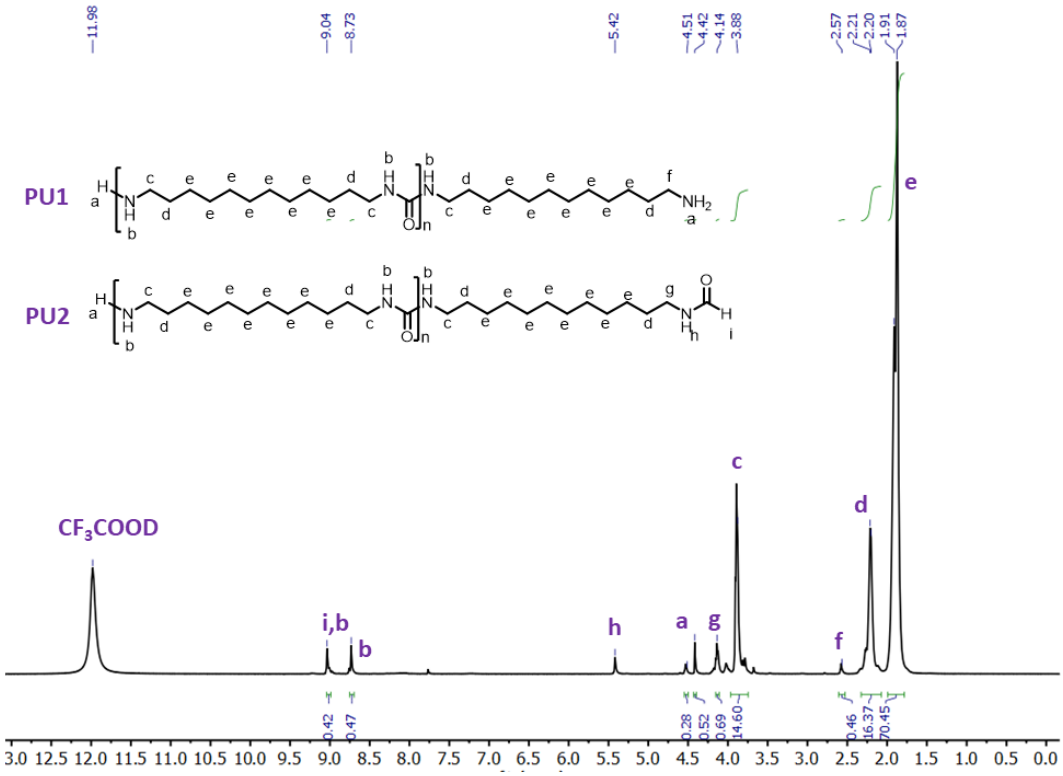

Figure S17. ^{1}H NMR spectrum (CF_3COOD, 500 MHz, 298 K) of the polyurea of the depicted structure.

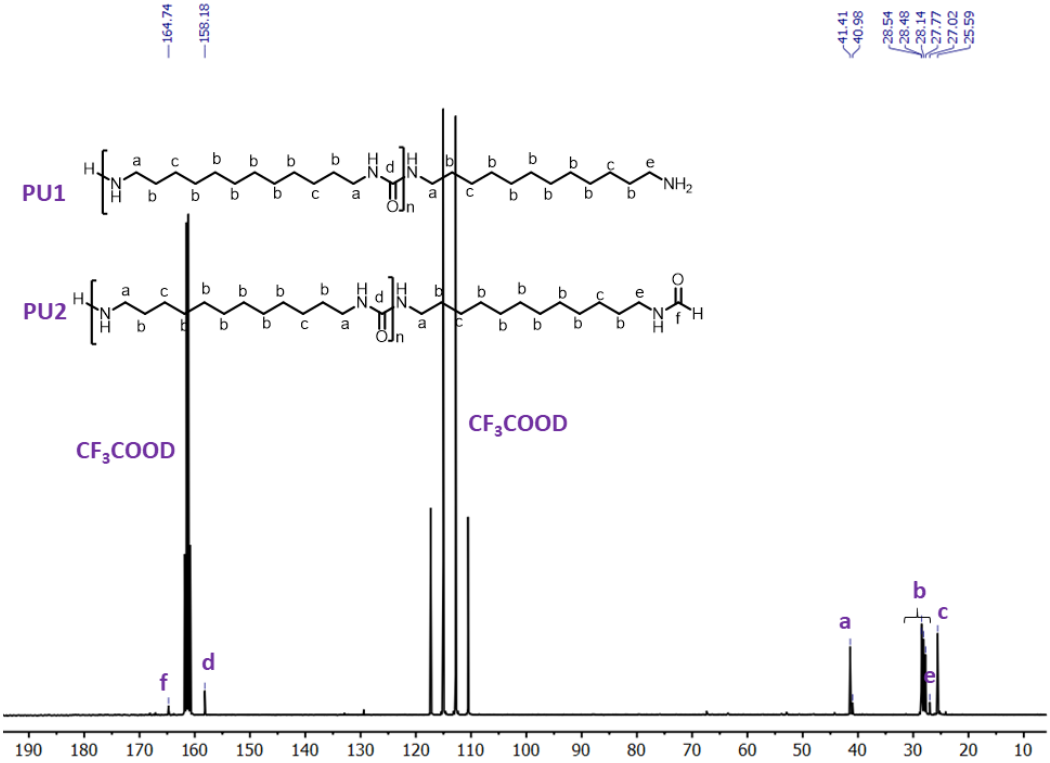

Figure S18. $^{13}C\{^{1}H\}$ NMR spectrum (CF_3COOD, 125 MHz, 298 K) of the polyurea of the depicted structure.

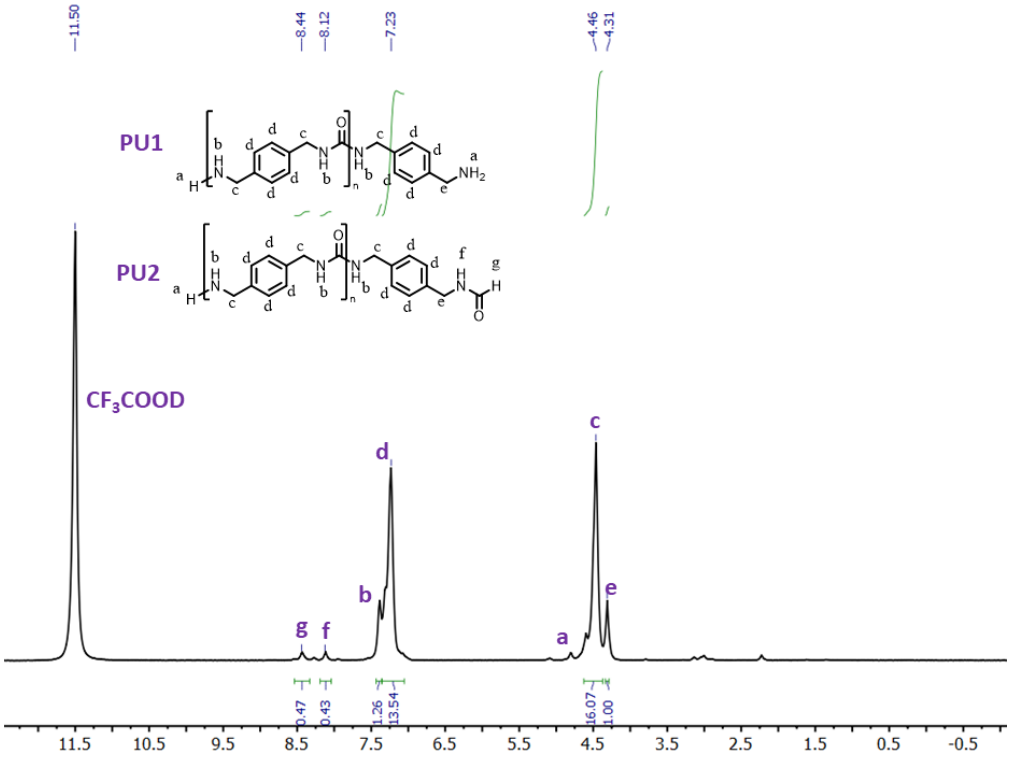

Figure S19. ^{1}H NMR spectrum (CF_3COOD, 500 MHz, 298 K) of the polyurea of the depicted structure.

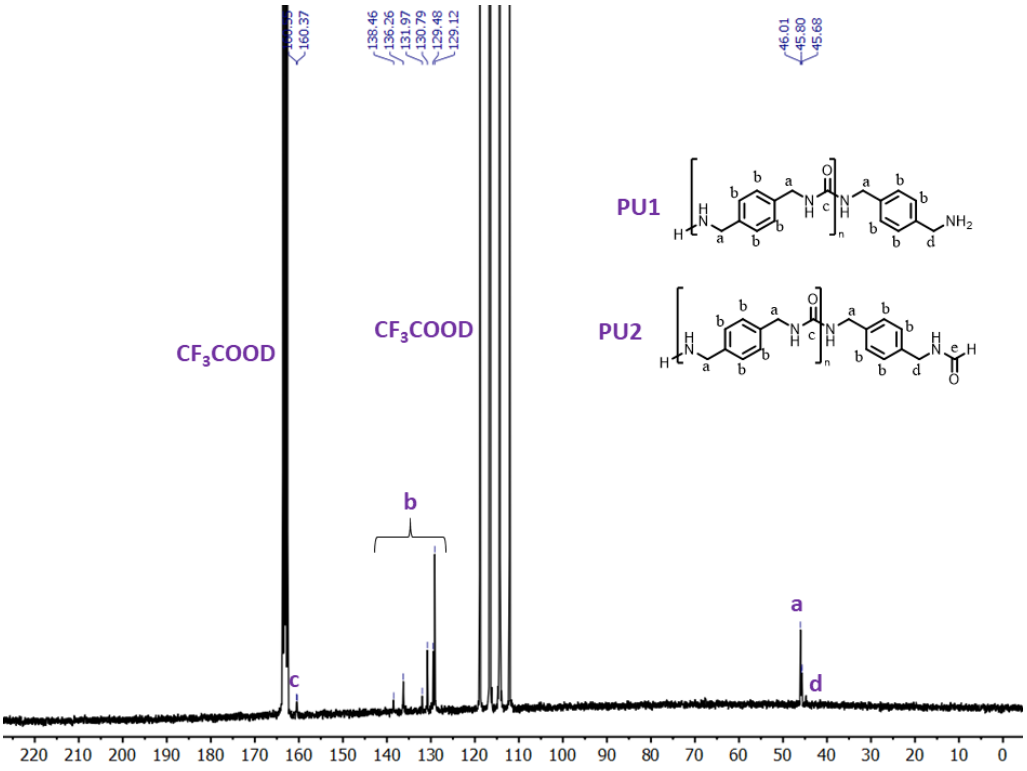

Figure S20. $^{13}C\{^{1}H\}$ NMR spectrum (CF_3COOD, 125 MHz, 298 K) of the polyurea of the depicted structure.

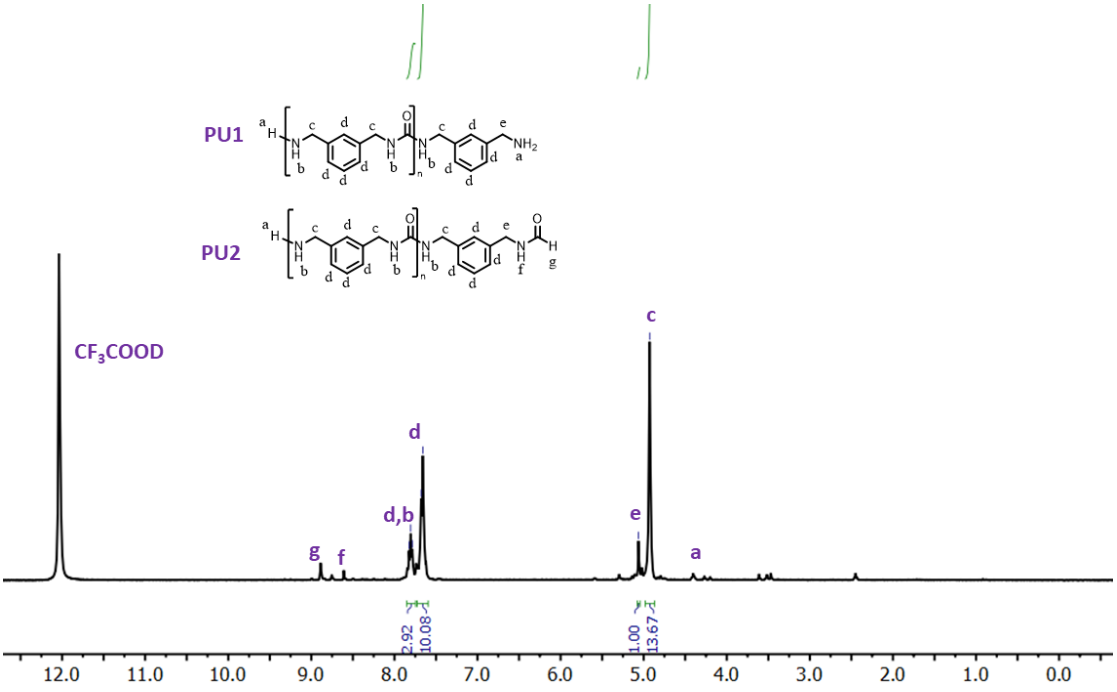

Figure S21. ^{1}H NMR spectrum (CF_3COOD, 500 MHz, 298 K) of the polyurea of the depicted structure.

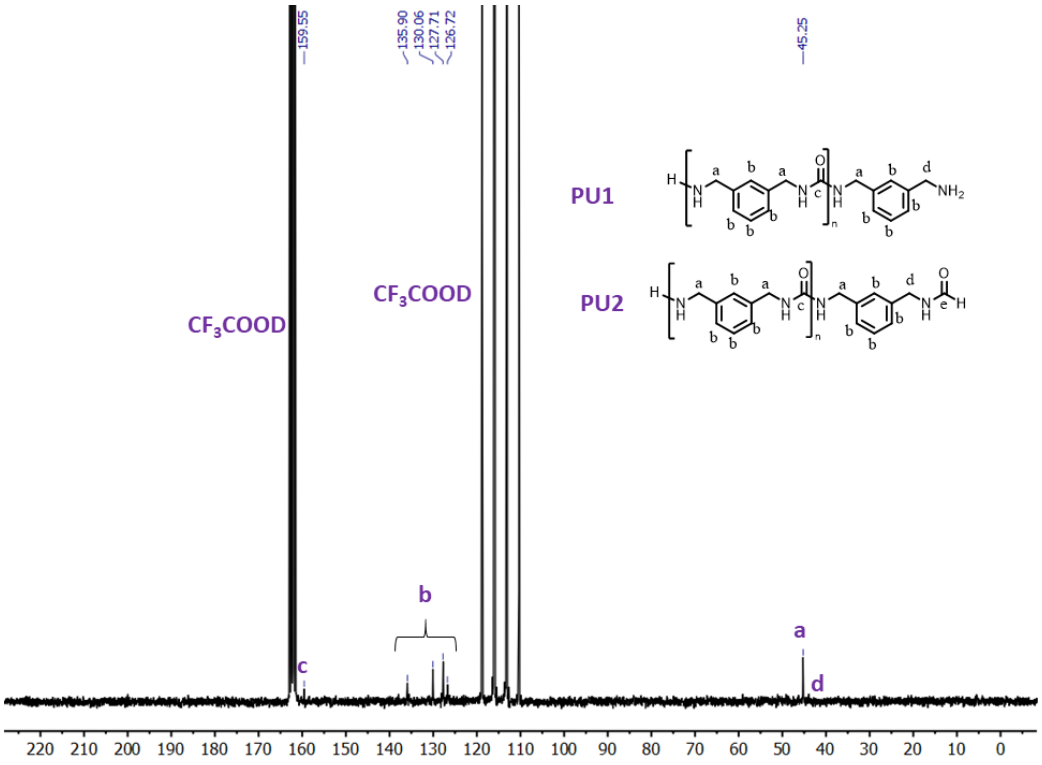

Figure S22. $^{13}C\{^{1}H\}$ NMR spectrum (CF_3COOD, 125 MHz, 298 K) of the polyurea of the depicted structure.

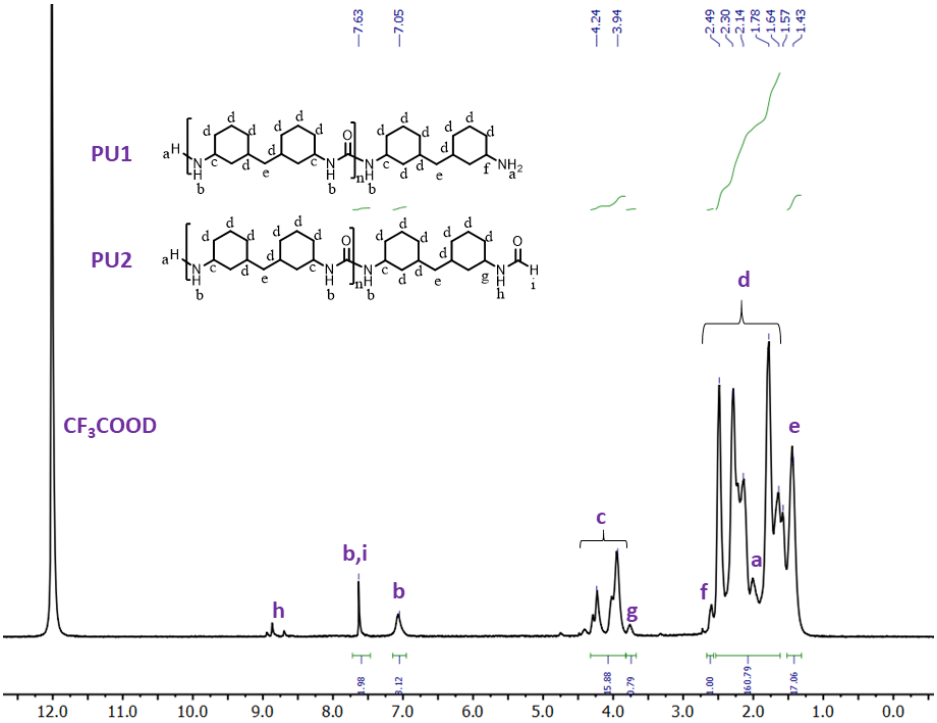

Figure S23. ^{1}H NMR spectrum (CF_3COOD, 500 MHz, 298 K) of the polyurea of the depicted structure.

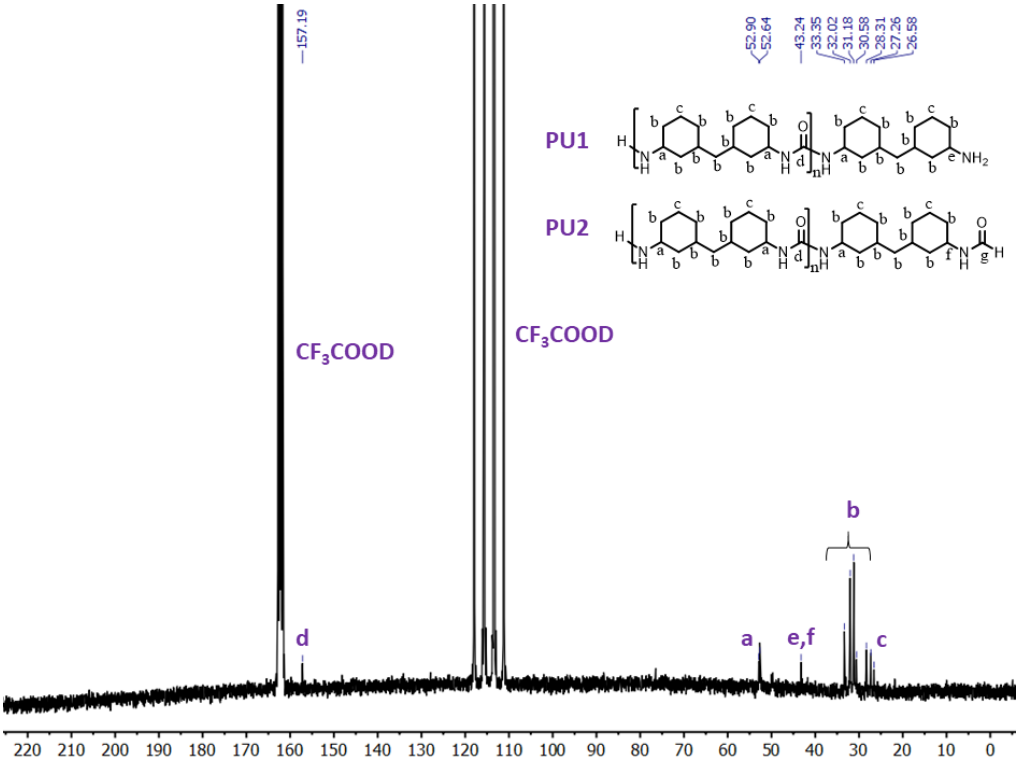

Figure S24. $^{13}C\{^{1}H\}$ NMR spectrum (CF_3COOD, 125 MHz, 298 K) of the polyurea of the depicted structure.

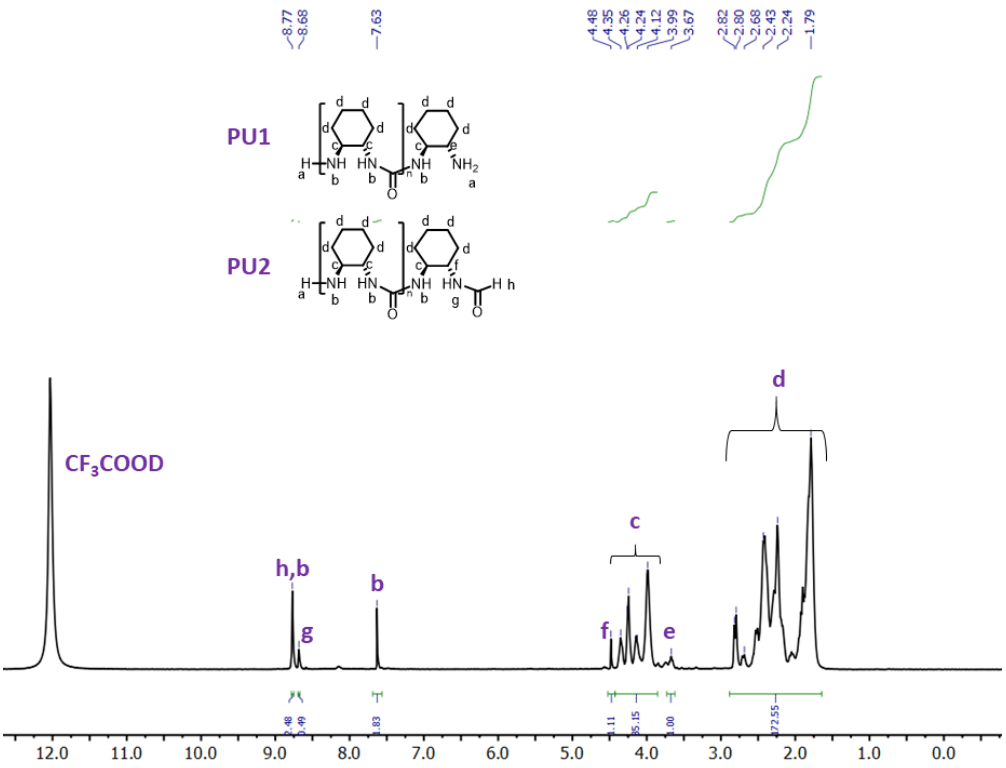

Figure S25. ^{1}H NMR spectrum (CF_3COOD, 500 MHz, 298 K) of the polyurea of the depicted structure.

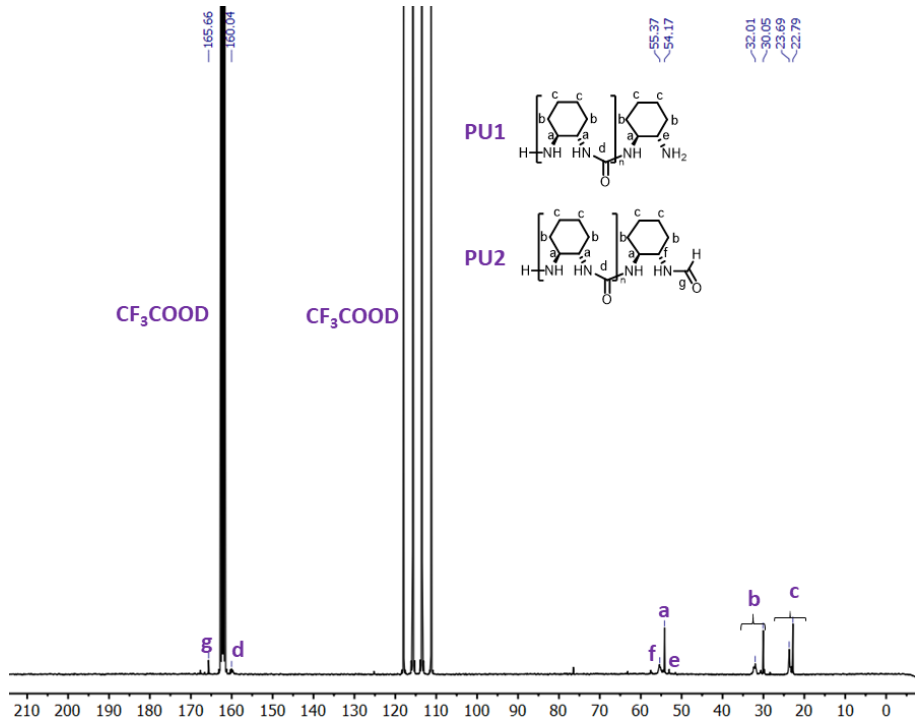

Figure S26. $^{13}C\{^{1}H\}$ NMR spectrum (CF_3COOD, 125 MHz, 298 K) of the polyurea of the depicted structure.

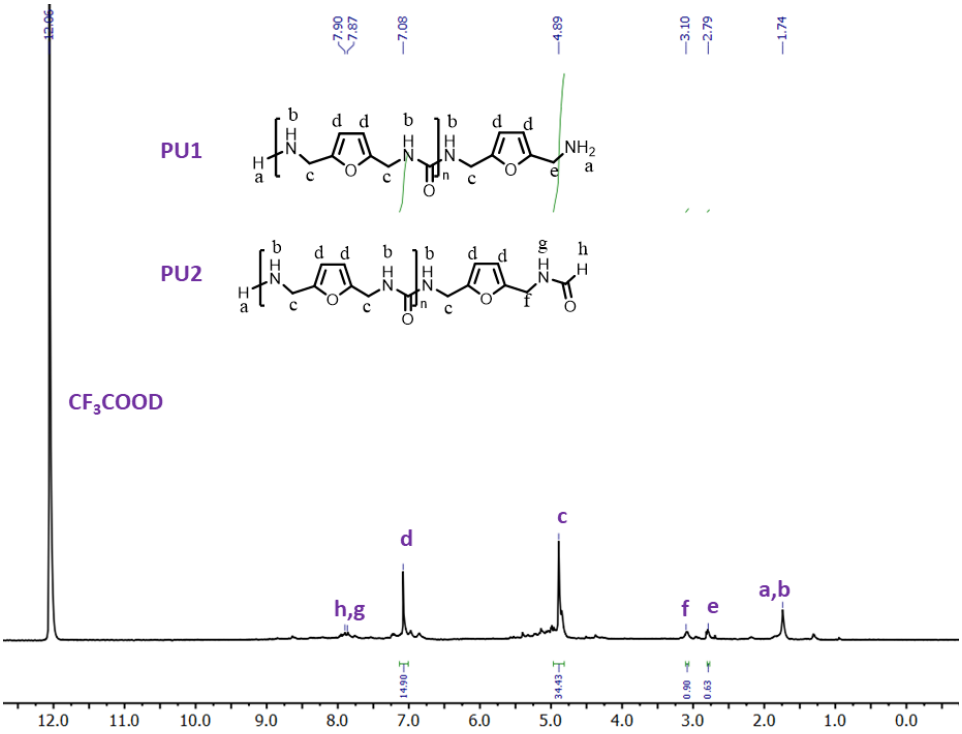

Figure S27. ^{1}H NMR spectrum (CF_3COOD, 500 MHz, 298 K) of the polyurea of the depicted structure.

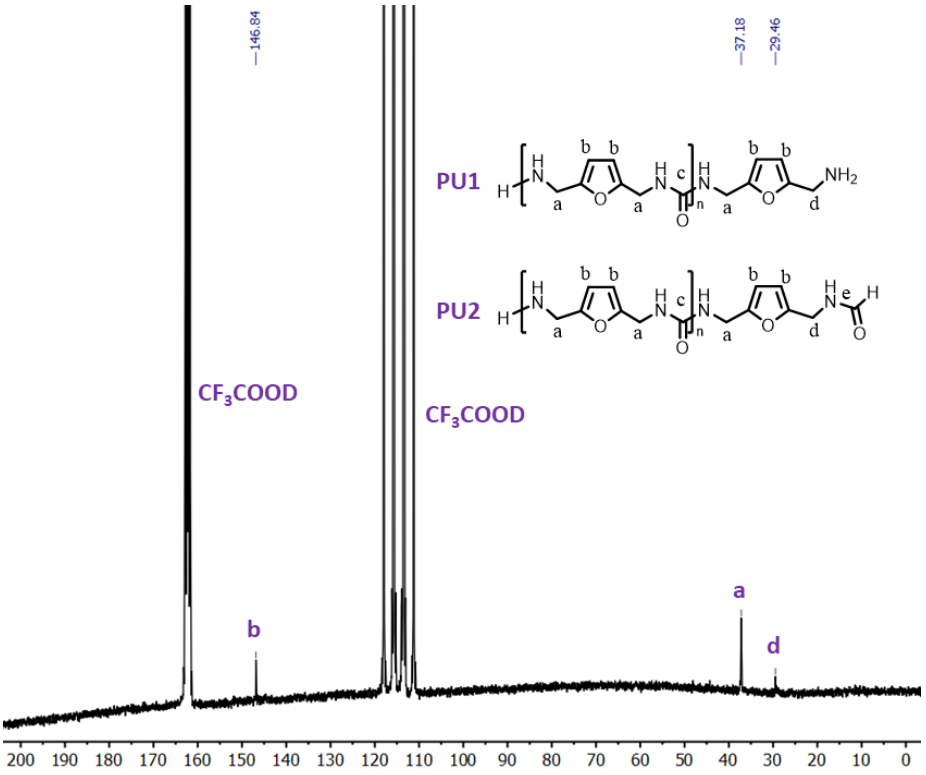

Figure S28. $^{13}C\{^{1}H\}$ NMR spectrum (CF_3COOD, 125 MHz, 298 K) of the polyurea of the depicted structure. The carbonyl signals were not observed due to the very poor solubility of the polyurea in CF_3COOD.

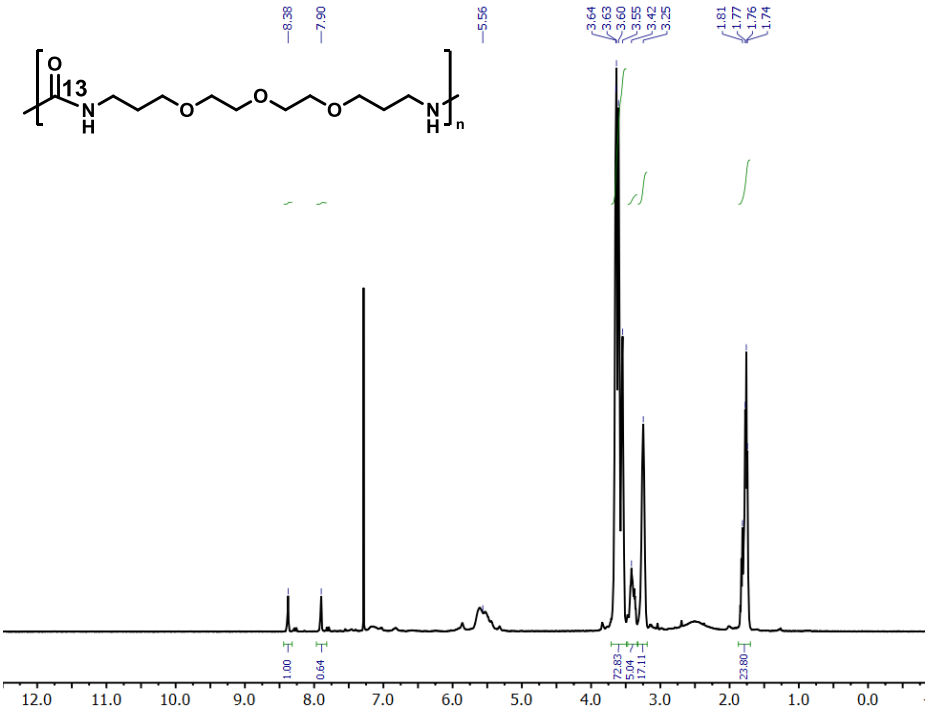

Figure S29. ^{1}H NMR spectrum ($CDCl_3$, 500 MHz, 298 K) of the ^{13}C-labelled polyurea of the depicted structure.

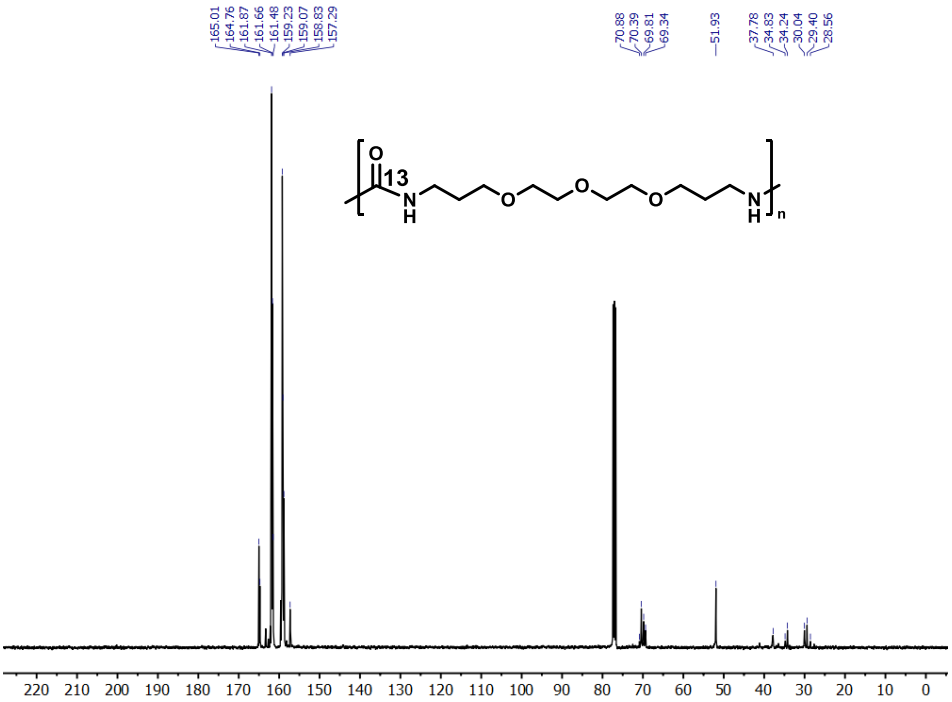

Figure S30. ^{13}C{^{1}H} NMR spectrum ($CDCl_3$, 125 MHz, 298 K) of the ^{13}C-labelled polyurea of the depicted structure.

10. IR spectra of the isolated polyureas

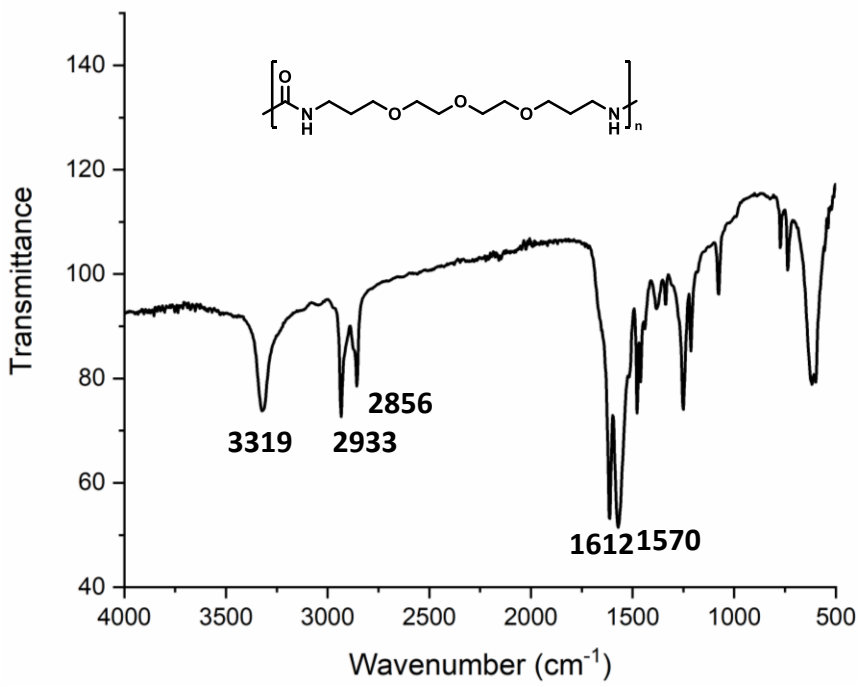

Figure S31. IR spectrum of the polyurea of the depicted structure.

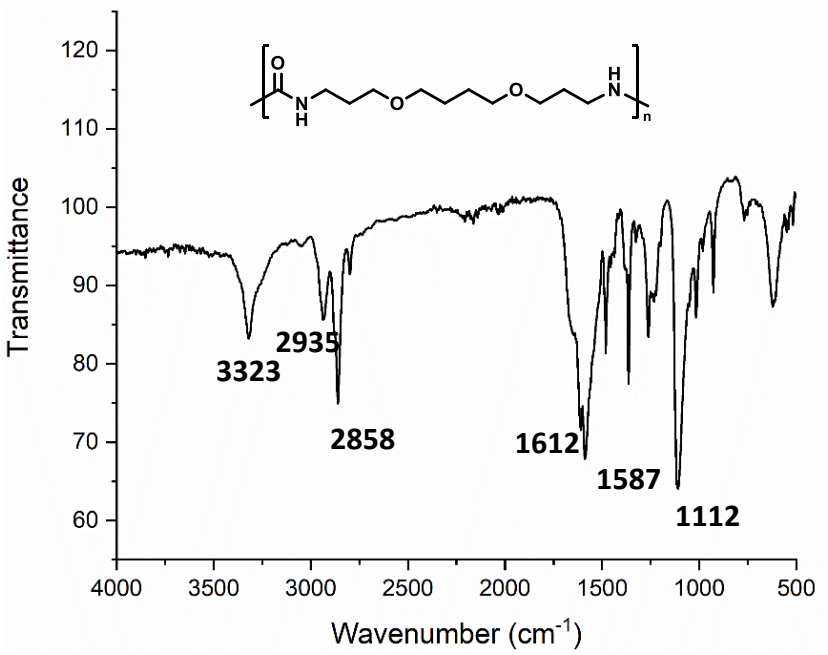

Figure S32. IR spectrum of the polyurea of the depicted structure.

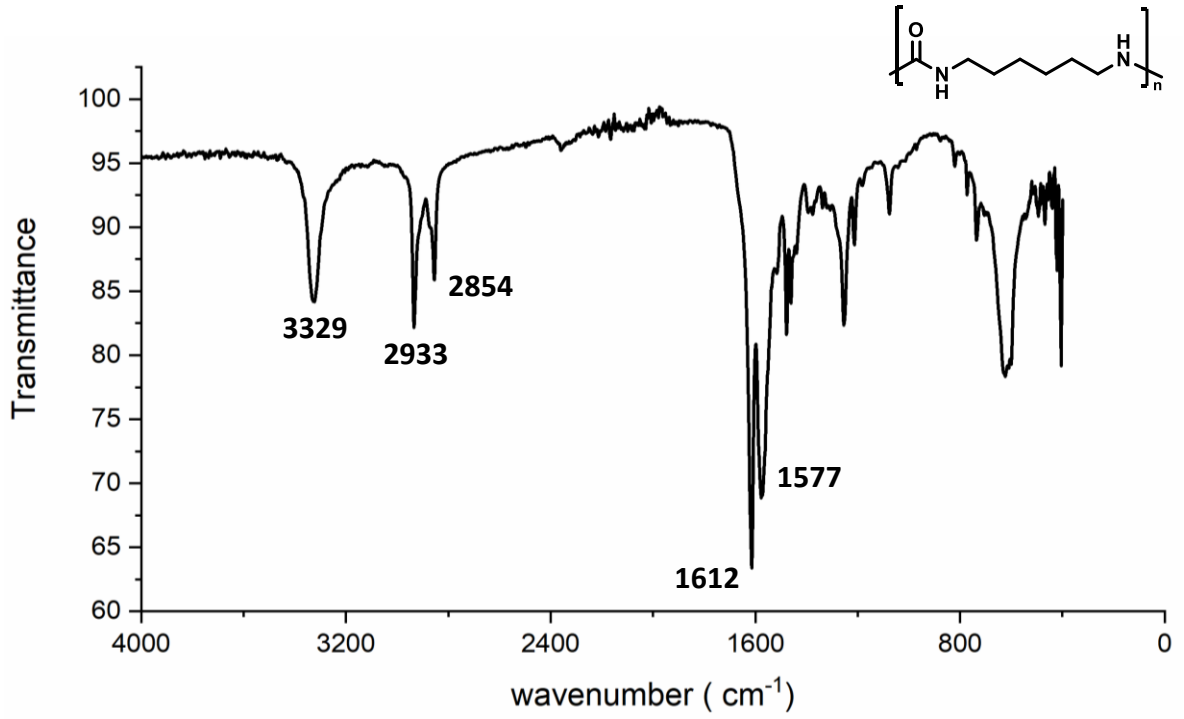

Figure S33. IR spectrum of the polyurea of the depicted structure.

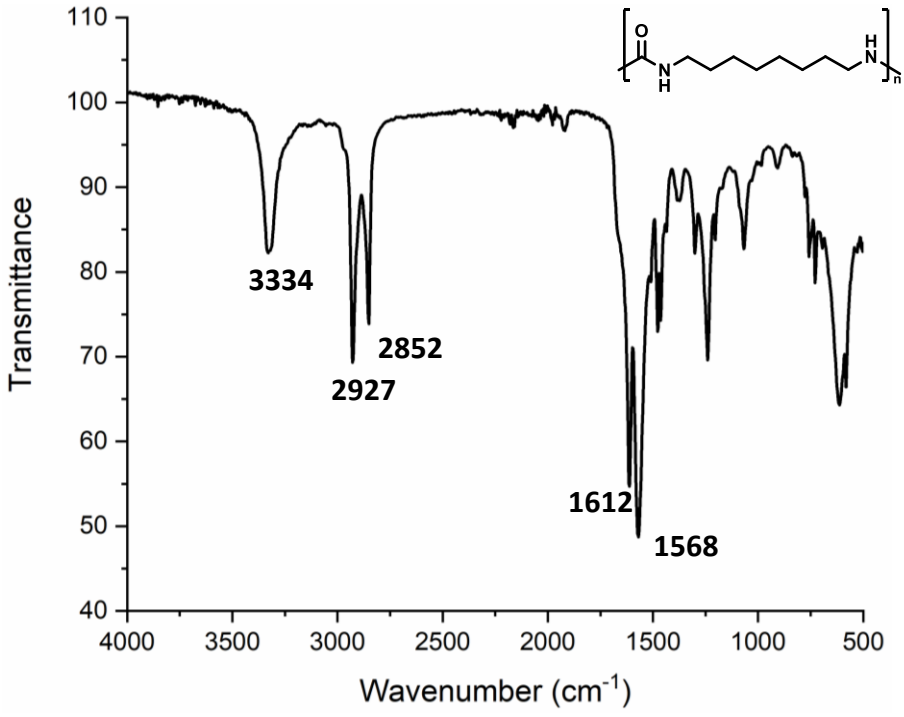

Figure S34. IR spectrum of the polyurea of the depicted structure.

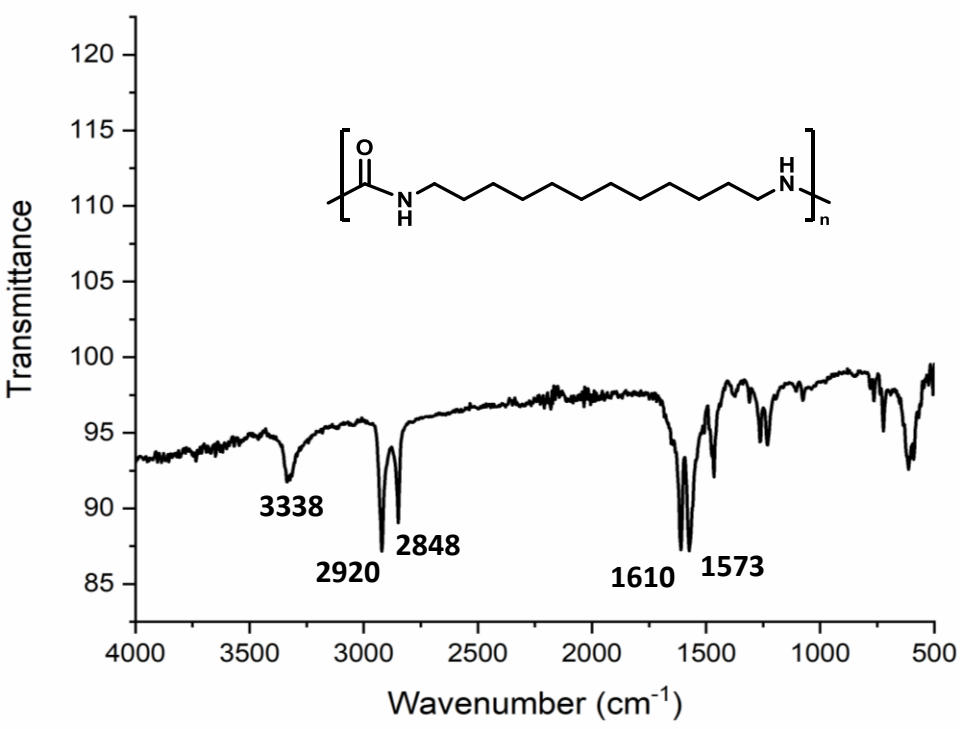

Figure S35. IR spectrum of the polyurea of the depicted structure.

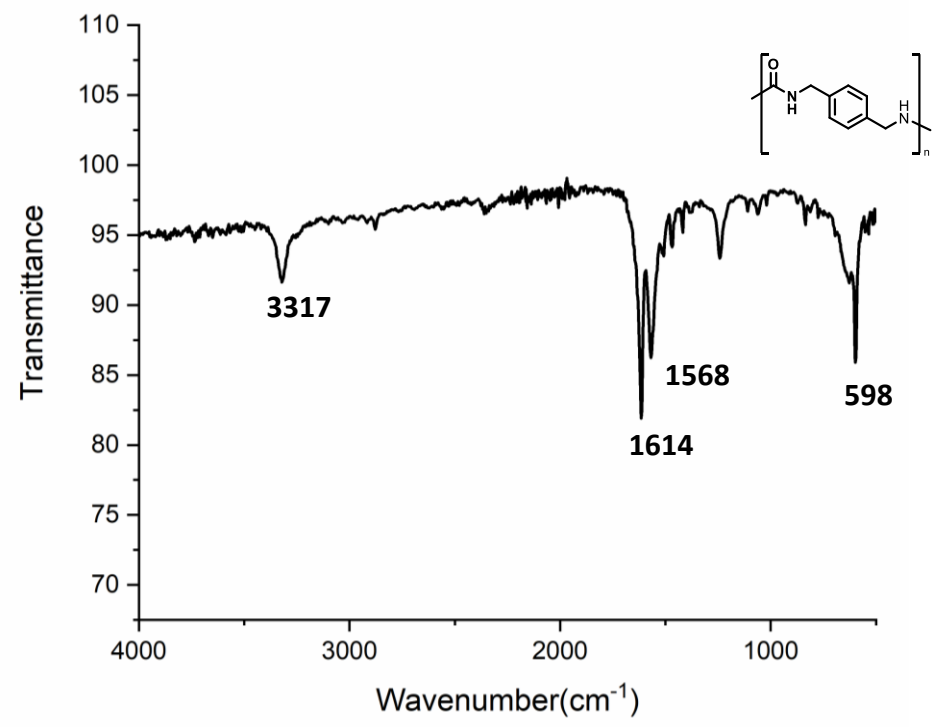

Figure S36. IR spectrum of the polyurea of the depicted structure.

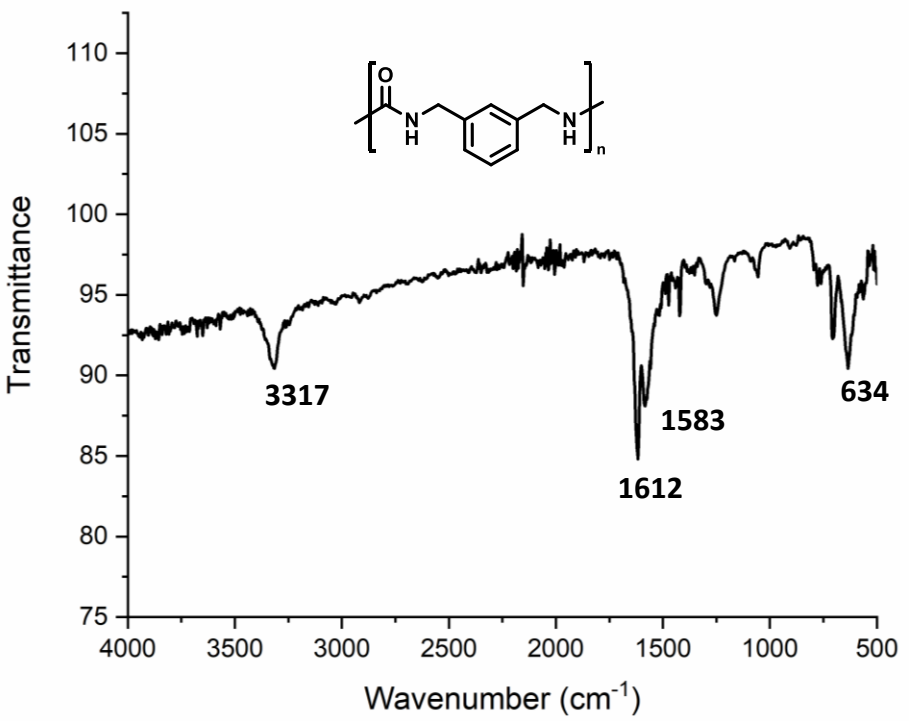

Figure S37. IR spectrum of the polyurea of the depicted structure.

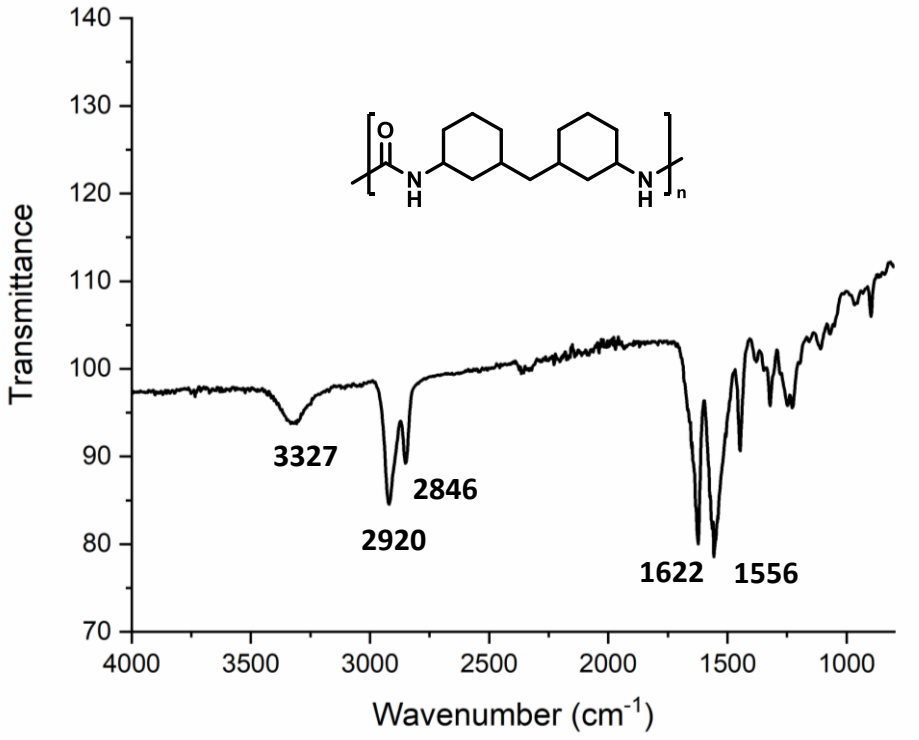

Figure S38. IR spectrum of the polyurea of the depicted structure.

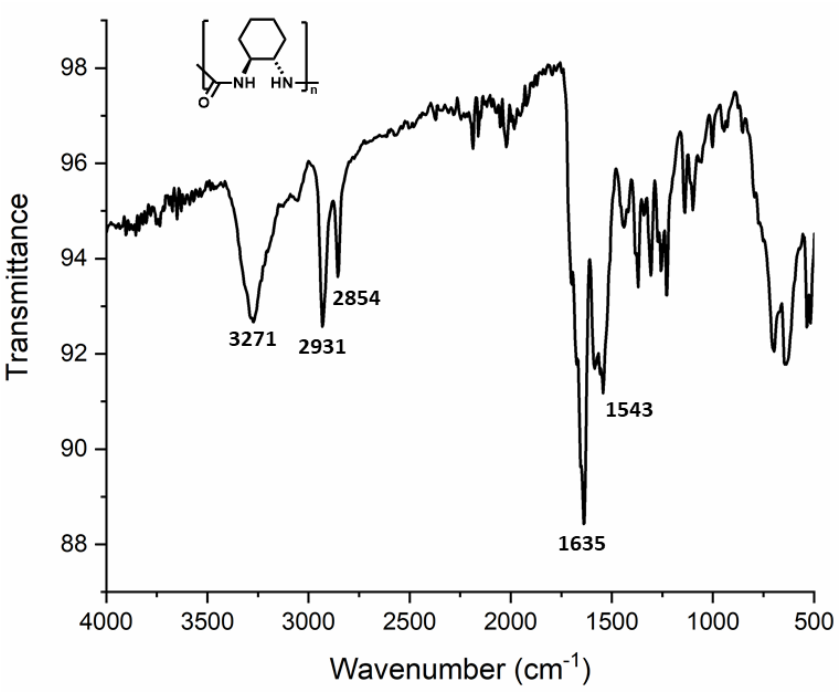

Figure S39. IR spectrum of the polyurea of the depicted structure.

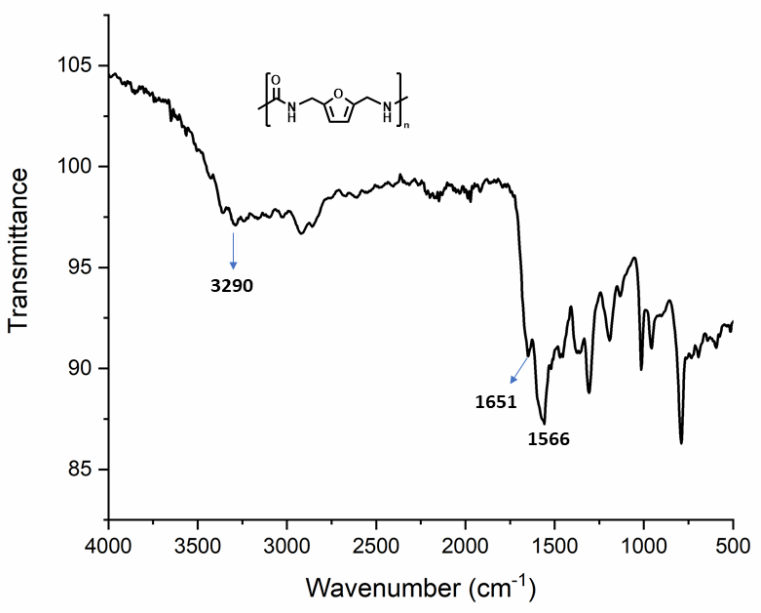

Figure S40. IR spectrum of the polyurea of the depicted structure.

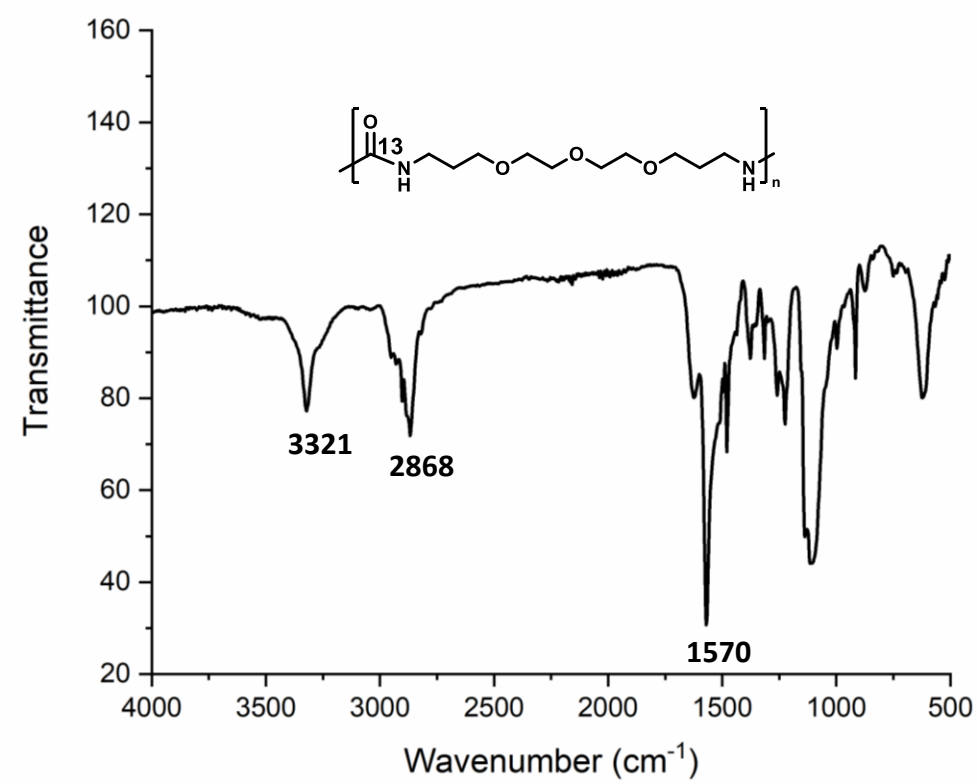

Figure S41. IR spectrum of the polyurea of the depicted structure.

11. Results of the MALDI-TOF mass spectrometry measurements

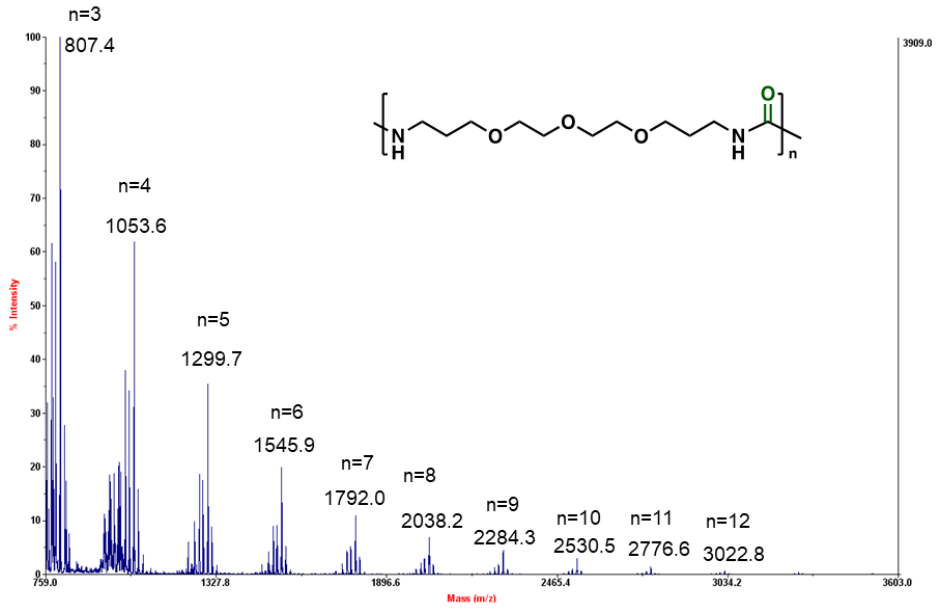

Figure S42. MALDI-TOF mass spectrum of the polyurea of the depicted structure. The masses represent the values corresponding to [M+K$^+$].

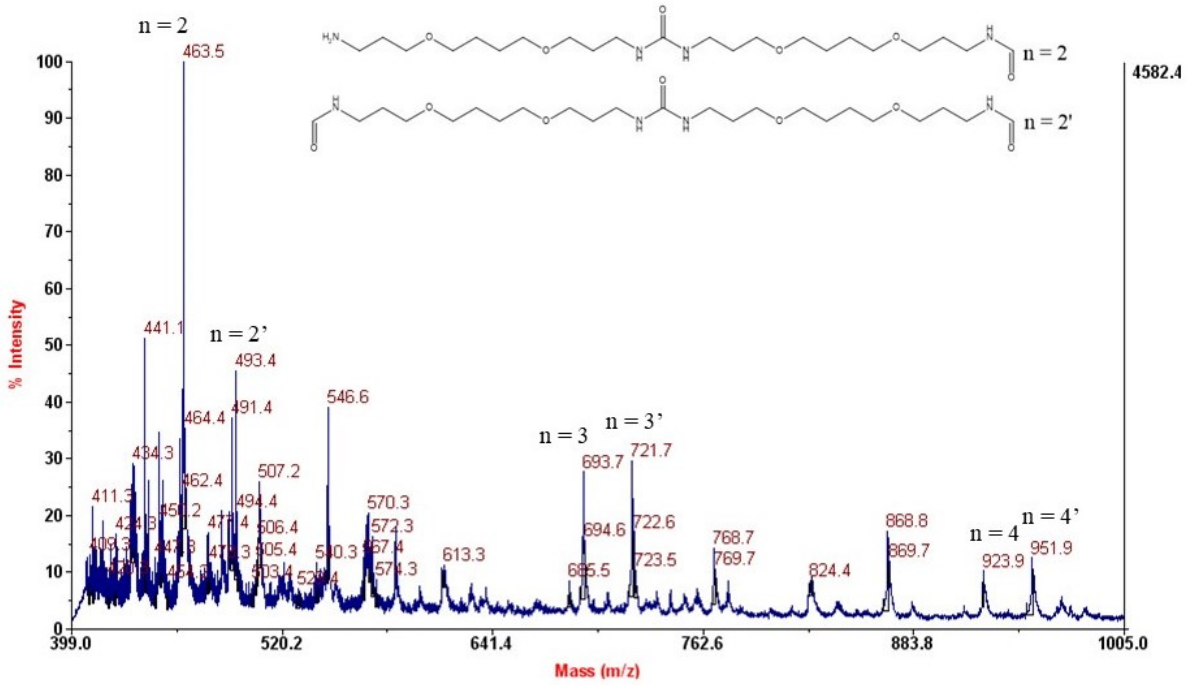

Figure S43. MALDI-TOF mass spectrum of the polyurea of the depicted structure. The masses represent the values corresponding to [M+H$^+$].

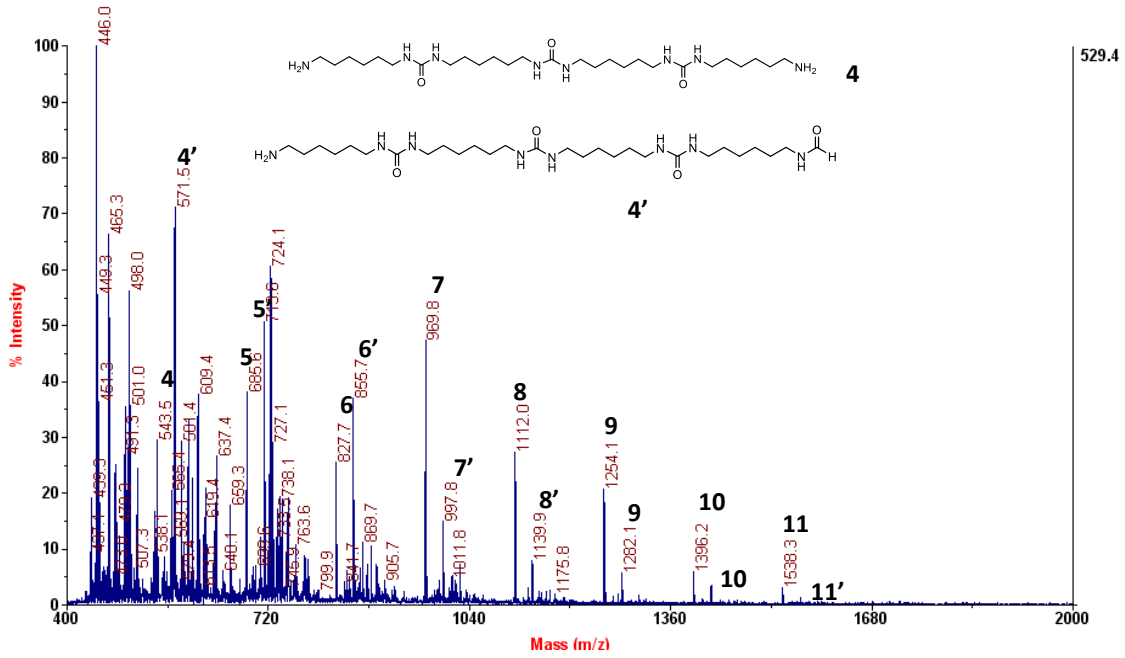

Figure S44. MALDI-TOF mass spectrum of the polyurea of the depicted structure. The masses represent the values corresponding to [M+H$^+$].

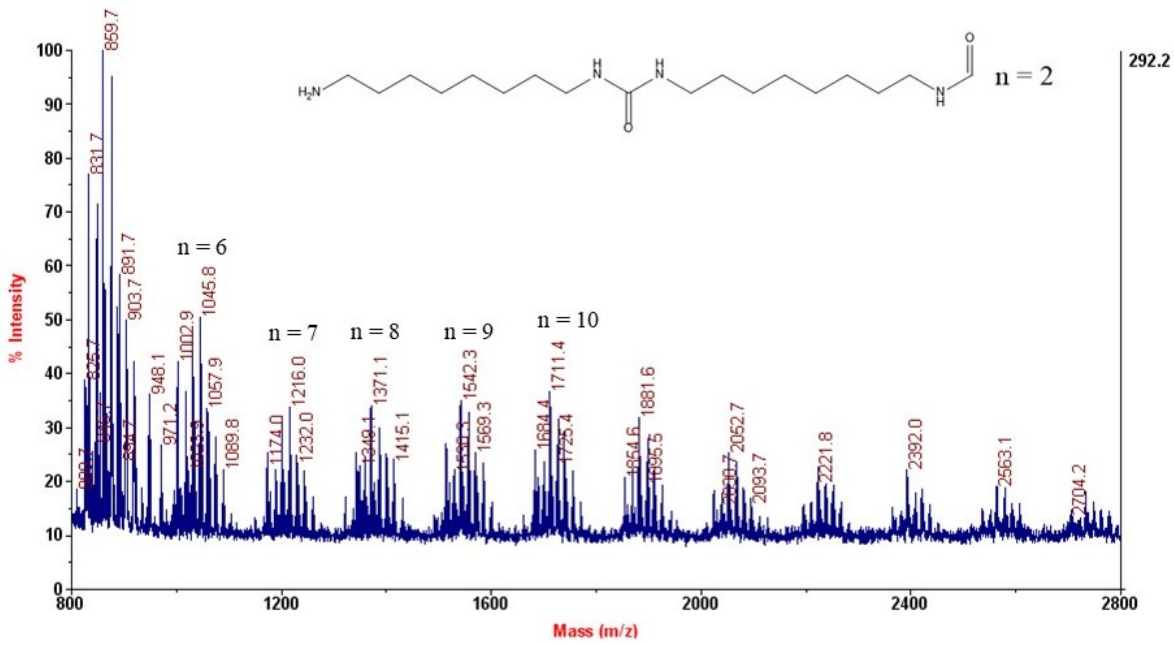

Figure S45. MALDI-TOF mass spectrum of the polyurea of the depicted structure. The masses represent the values corresponding to [M+K$^+$].

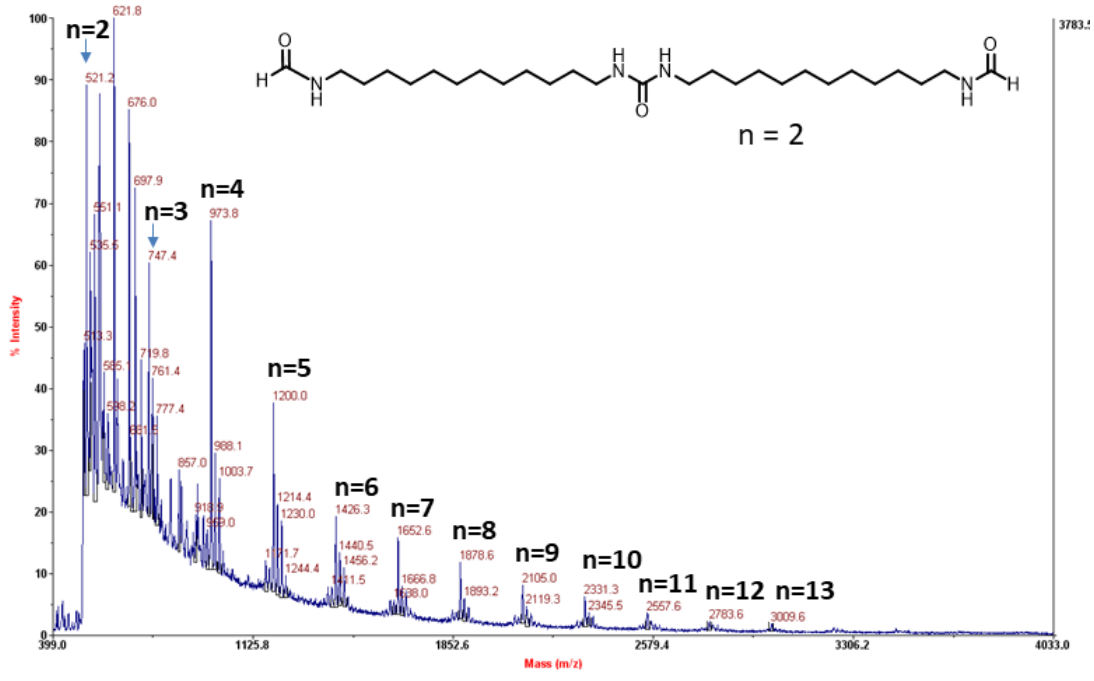

Figure S46. MALDI-TOF mass spectrum of the polyurea of the depicted structure. The masses represent the values corresponding to [M+K$^+$].

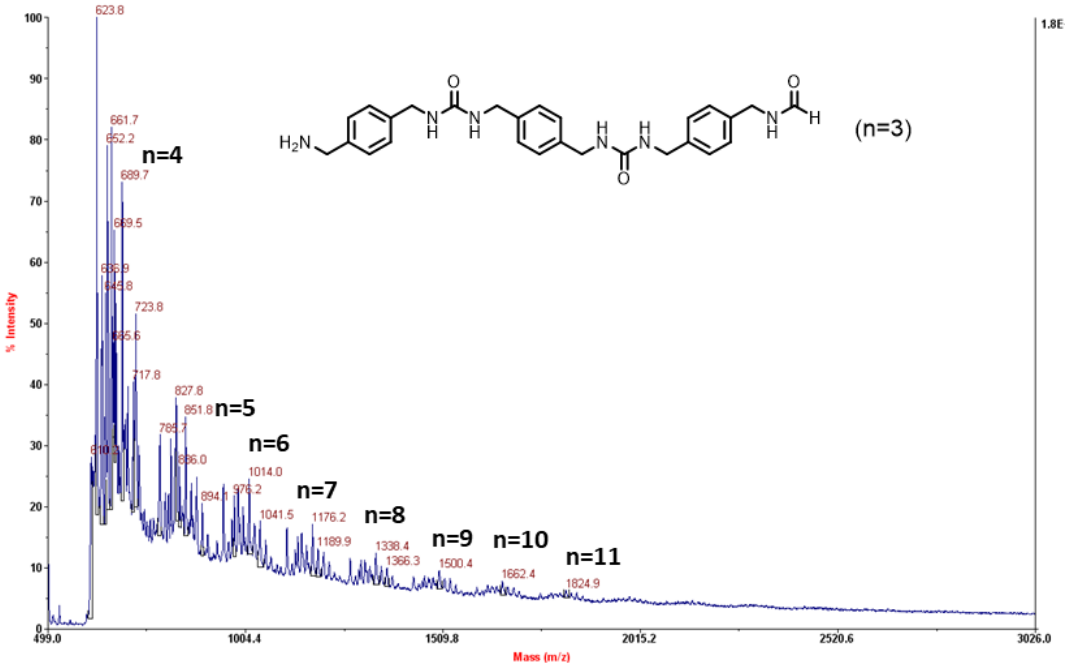

Figure S47. MALDI-TOF mass spectrum of the polyurea of the depicted structure. The masses represent the values corresponding to [M+K$^+$].

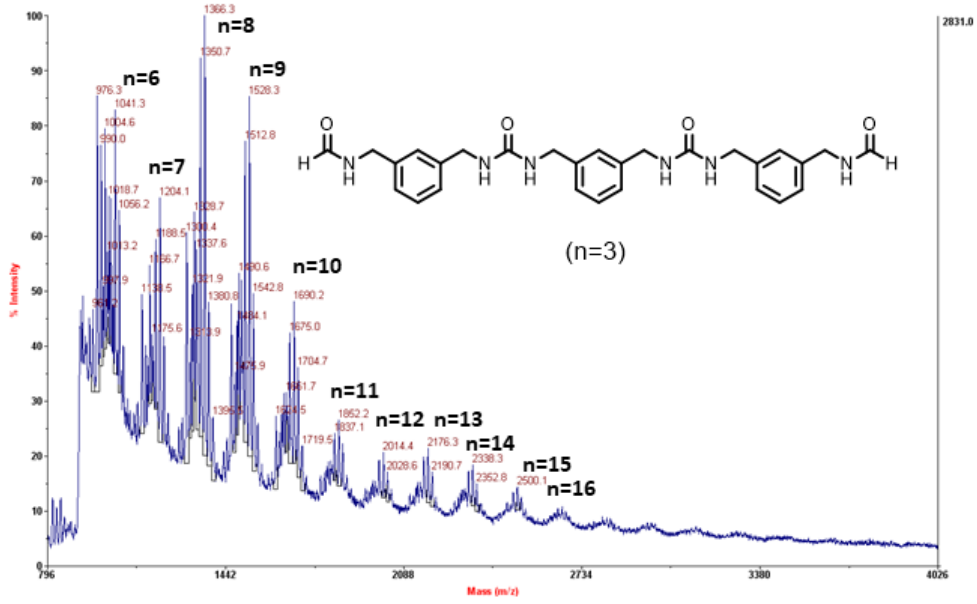

Figure S48. MALDI-TOF mass spectrum of the polyurea of the depicted structure. The masses represent the values corresponding to [M+H$^+$].

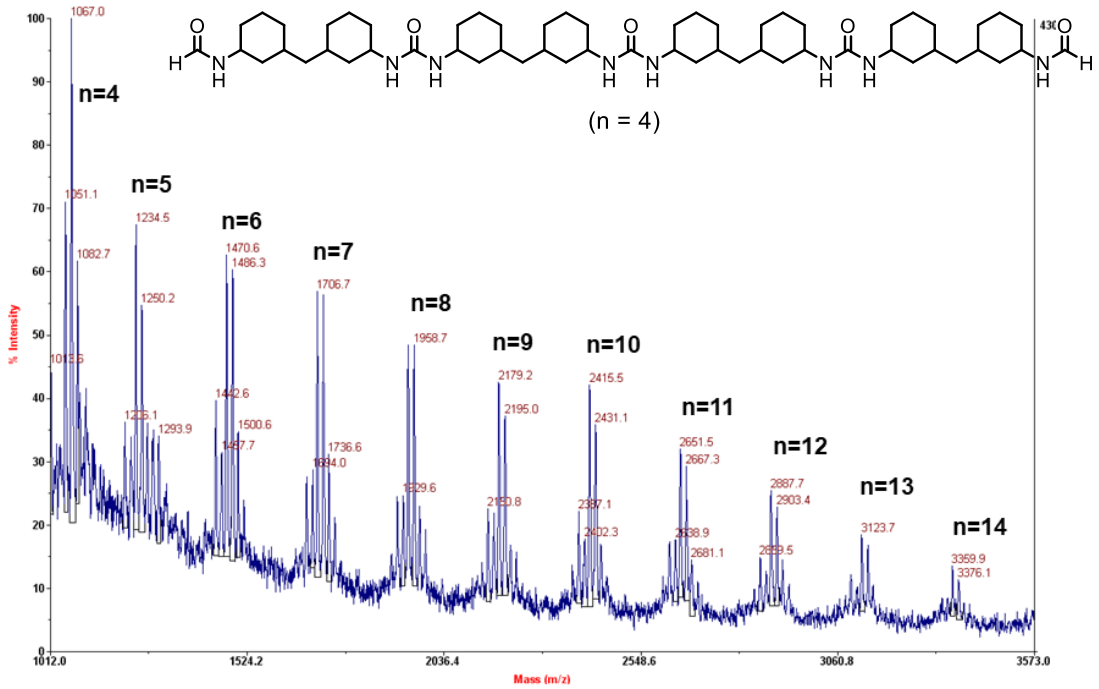

Figure S49. MALDI-TOF mass spectrum of the polyurea of the depicted structure. The masses represent the values corresponding to [M+K$^+$].

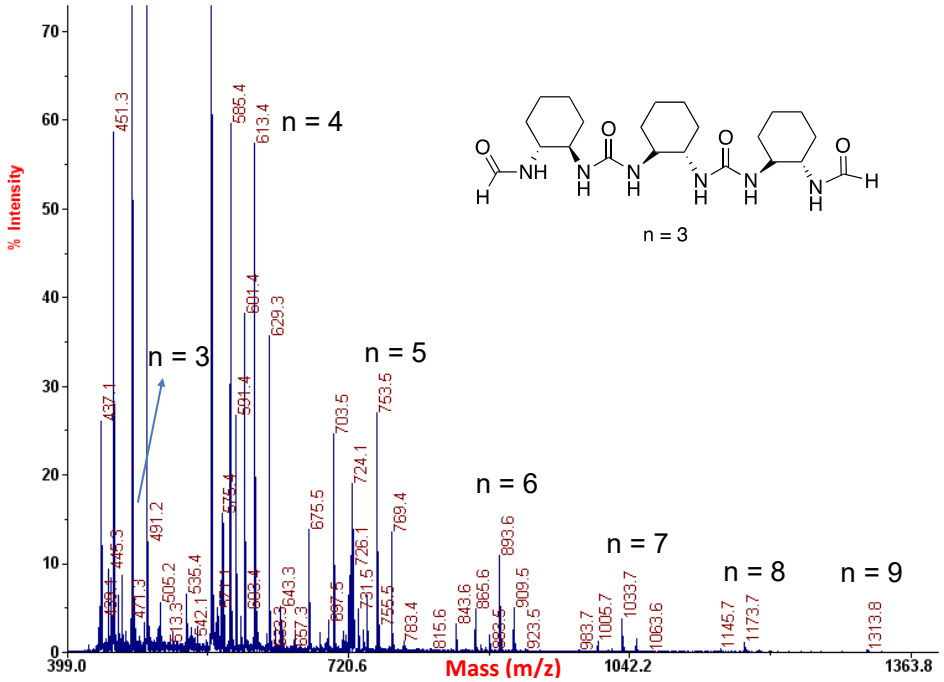

Figure S50. MALDI-TOF mass spectrum of the polyurea of the depicted structure. The masses represent the values corresponding to [M+Na$^+$].

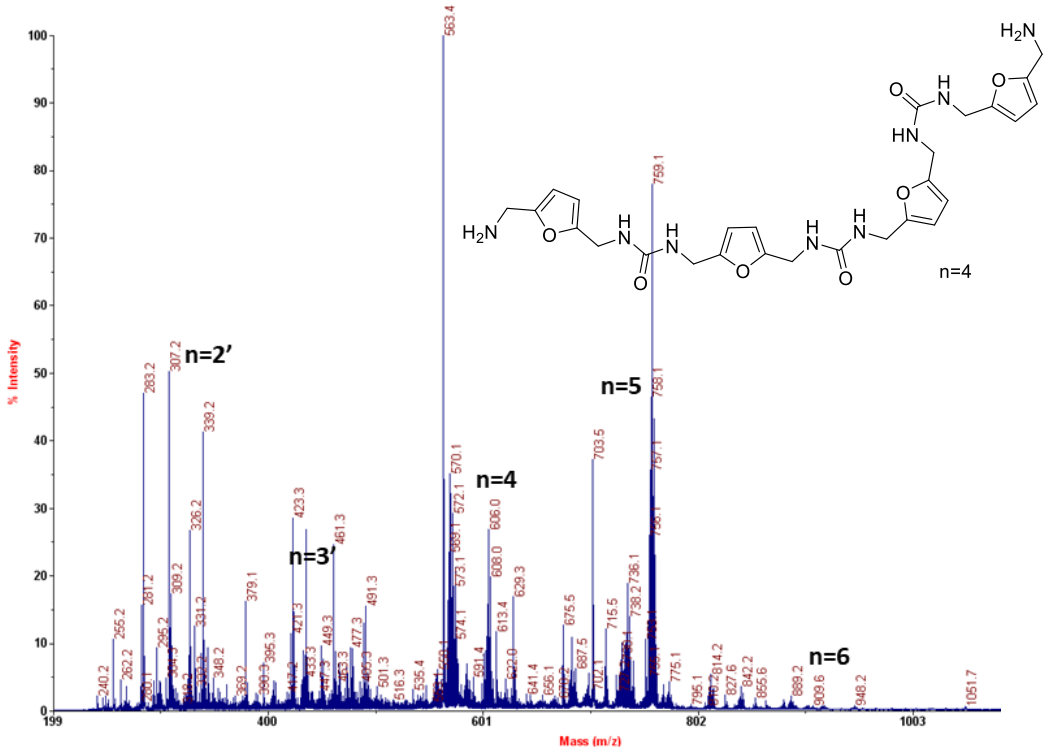

Figure S51. MALDI-TOF mass spectrum of the polyurea of the depicted structure. The masses represent the values corresponding to [M+H$^+$] for n = 2-3, and [M+Na$^+$] for n =4-6. The sample exhibited very poor solubility in TFA because of which higher oligomers were not observed presumably.

12. Comparison of the IR and MALDI data for the unlabeled and labelled polyurea

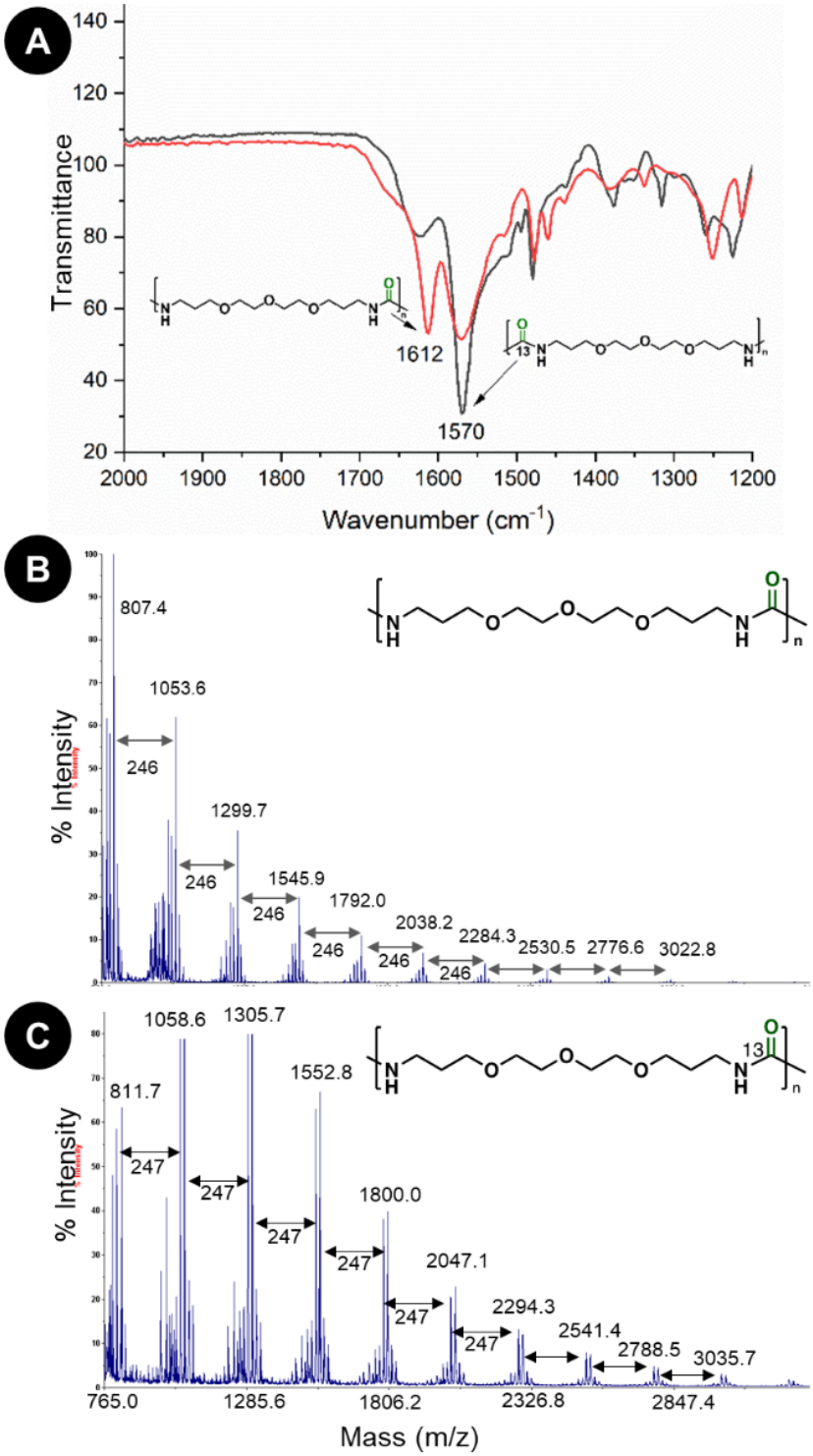

Figure S52. IR spectra (1200-2000 cm^{-1} region) showing carbonyl stretching frequency of the ^{13}C-labelled and the unlabeled polyurea (**A**). MALDI-TOF mass spectra for the unlabeled (**B**) and the ^{13}C-labelled polyurea (**C**). The masses represent the values corresponding to $[M+K^+]$.

13. Results of the TGA measurements

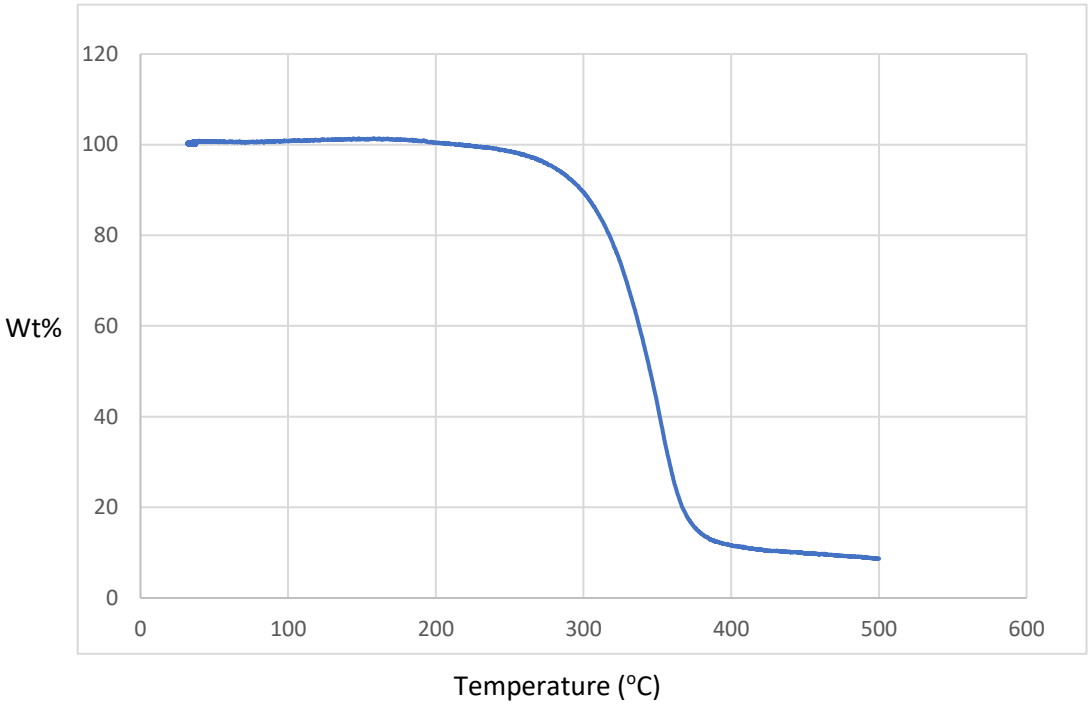

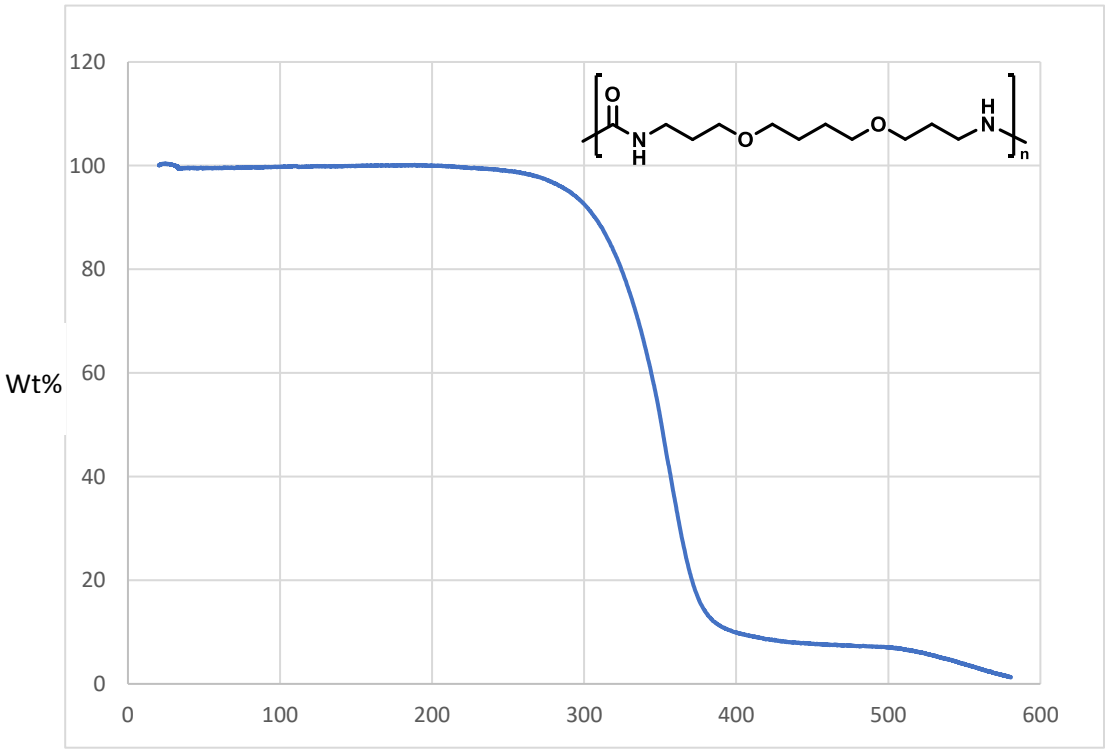

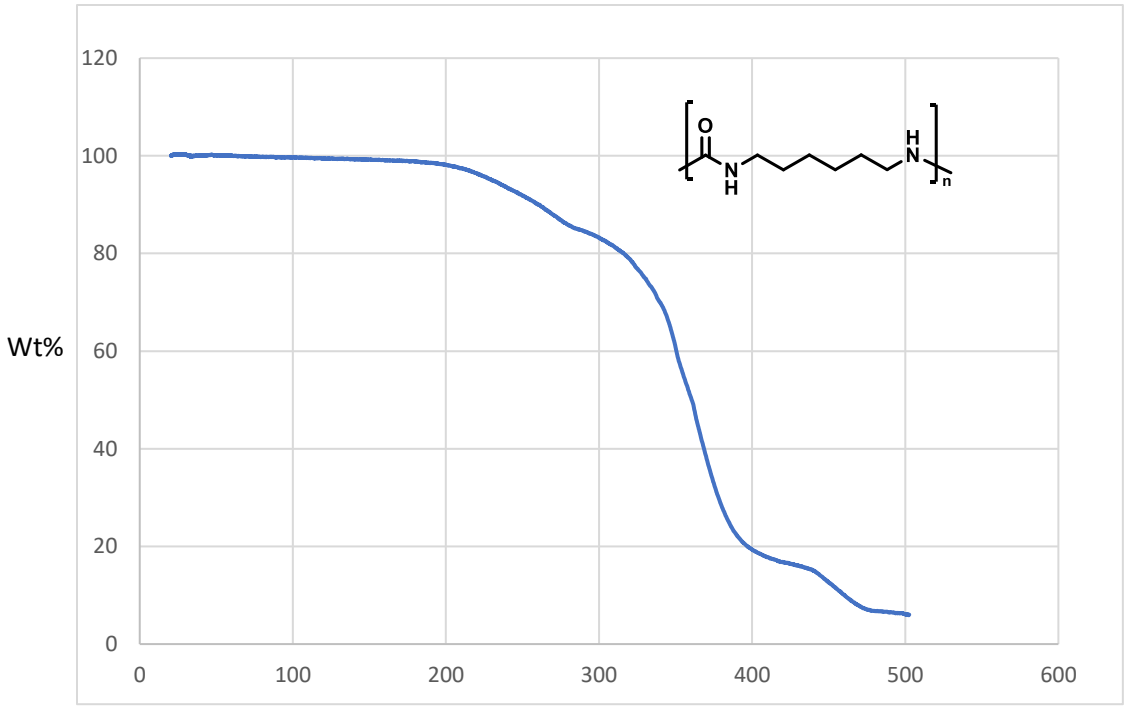
120
100
80
60
40
20
0
Wt%
0
100
200
300
400
500
600
Temperature (°C)

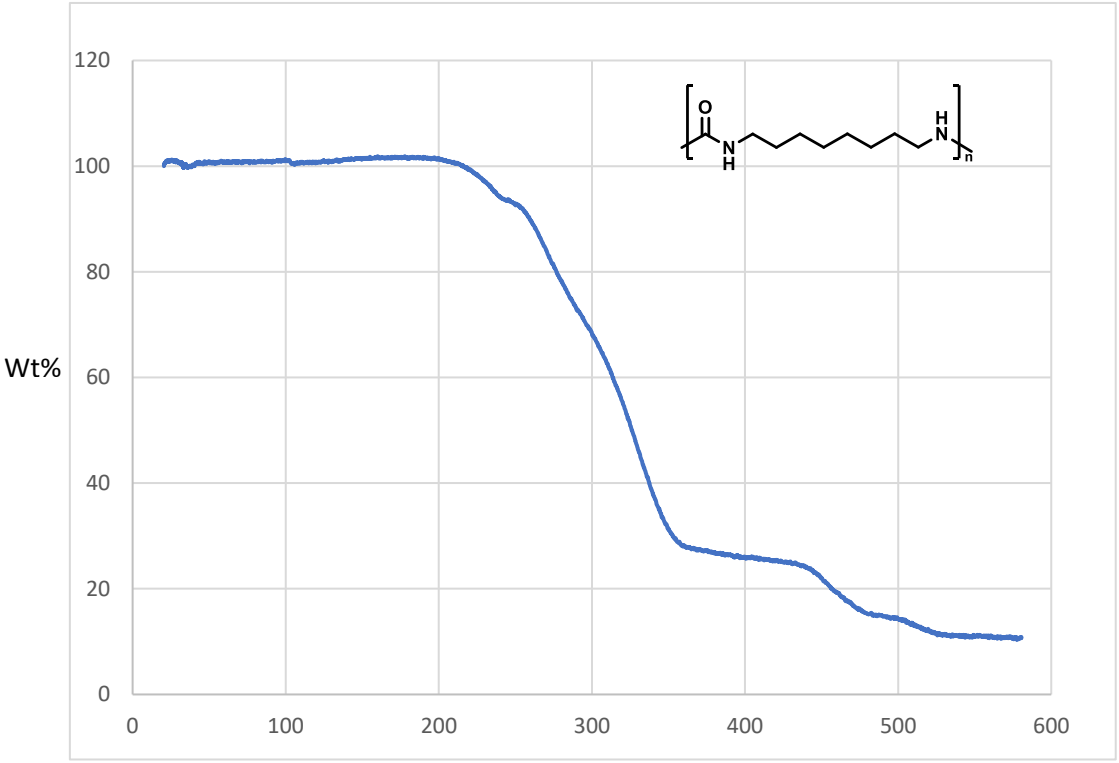
120
100
80
60
40
20
0
Wt%
0
100
200
300
400
500
600
Temperature (°C)

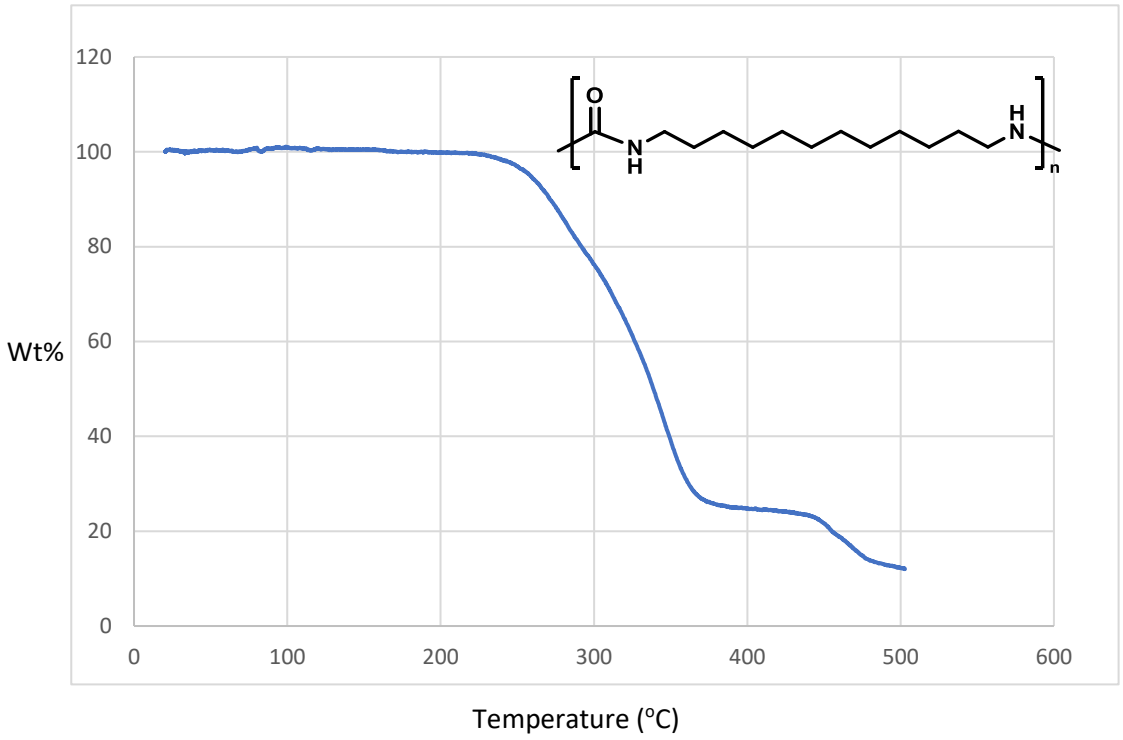
120
100
80
60
40
20
0
Wt%
0
100
200
300
400
500
600
Temperature (°C)

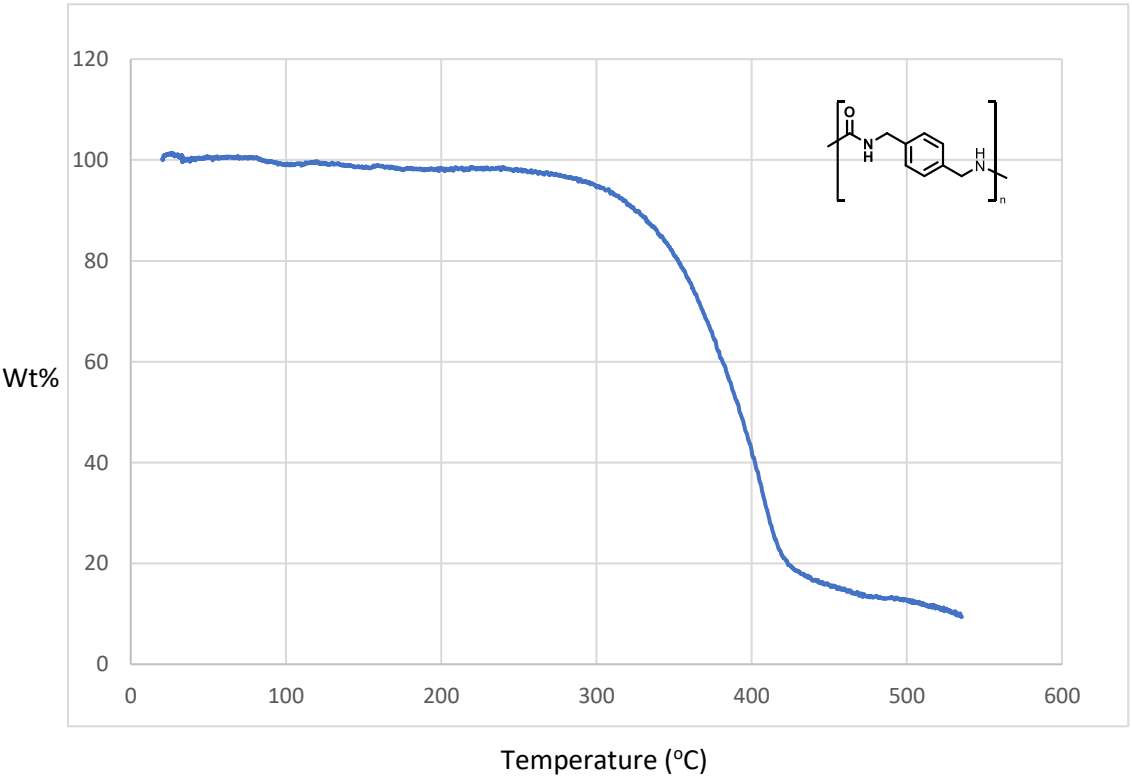
120
100
80
60
40
20
0
Wt%
0
100
200
300
400
500
600
Temperature (°C)

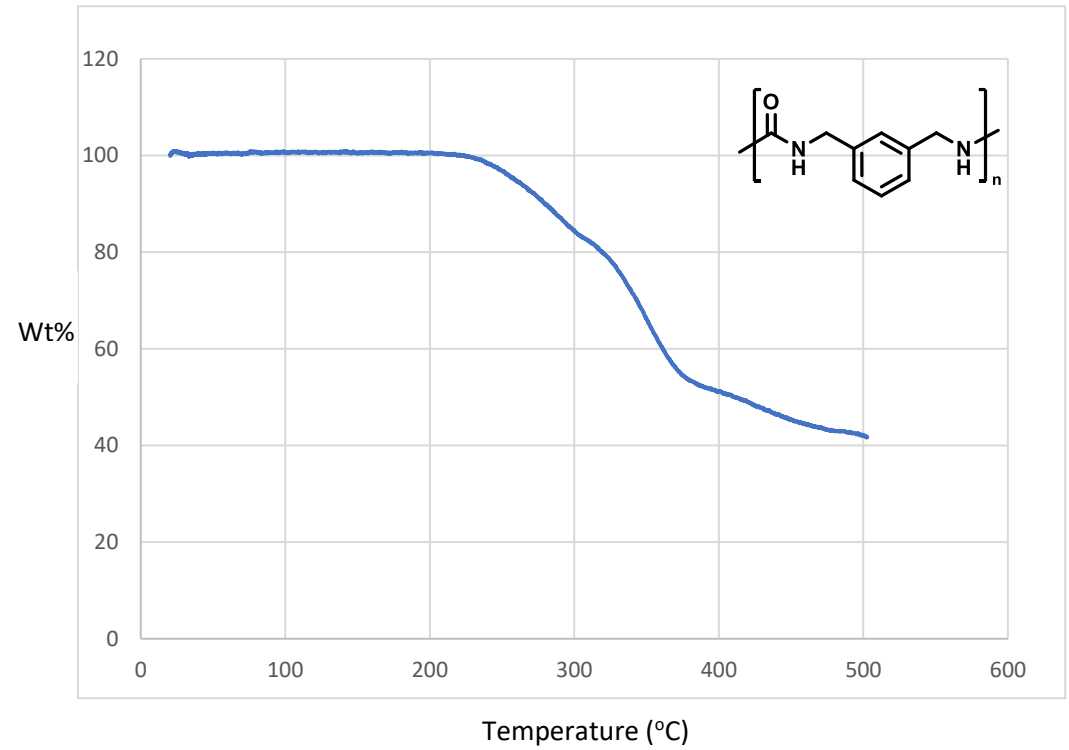
120
100
80
60
40
20
0
Wt%
0
100
200
300
400
500
600
Temperature (°C)

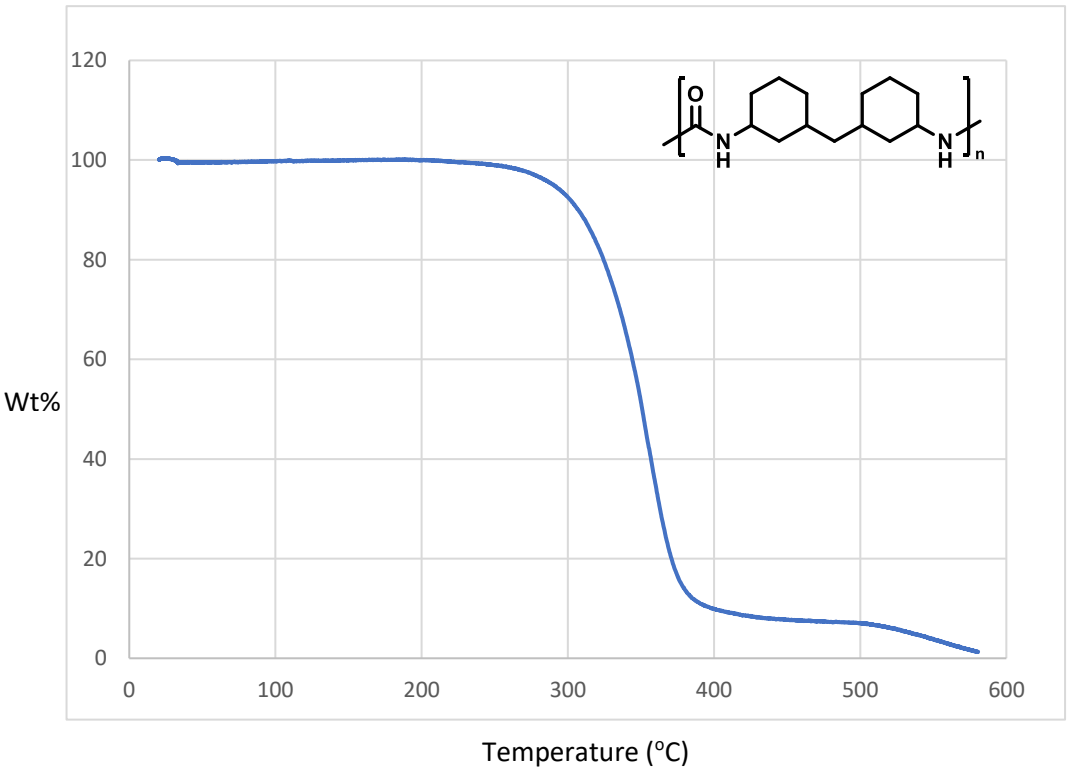
120
100
80
60
40
20
0
Wt%
0
100
200
300
400
500
600
Temperature (°C)

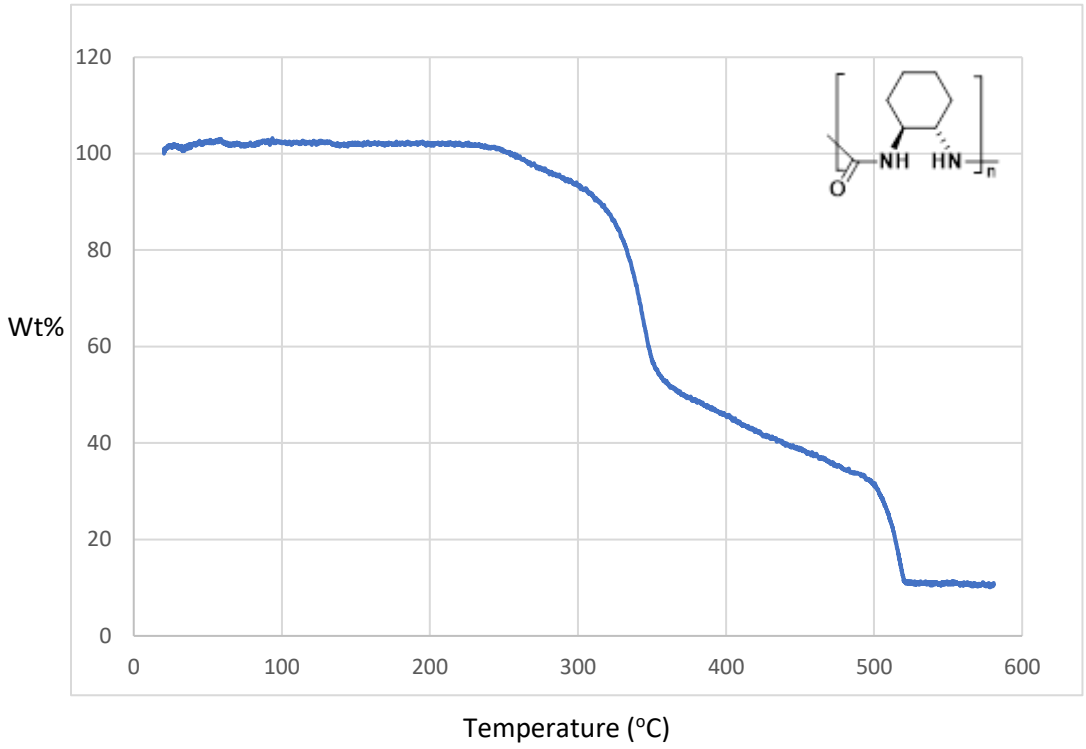
120
100
80
60
40
20
0
Wt%
0
100
200
300
400
500
600
Temperature (°C)
NH
HN
n
O

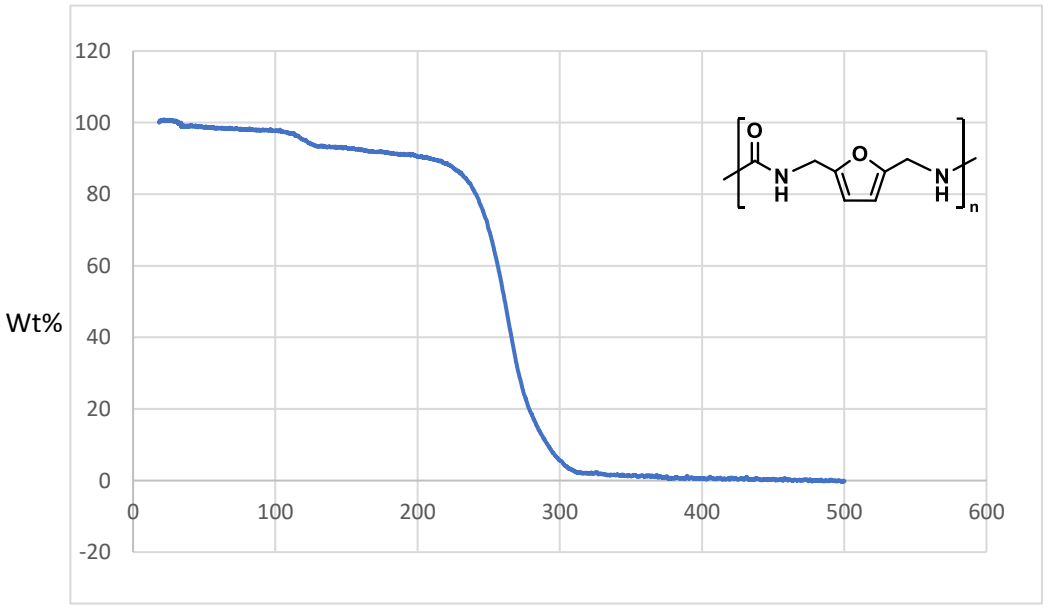
120
100
80
60
40
20
0
-20
Wt%
0
100
200
300
400
500
600
Temperature (°C)
O
N
H
O
N
H
n

14. Results of the DSC measurements

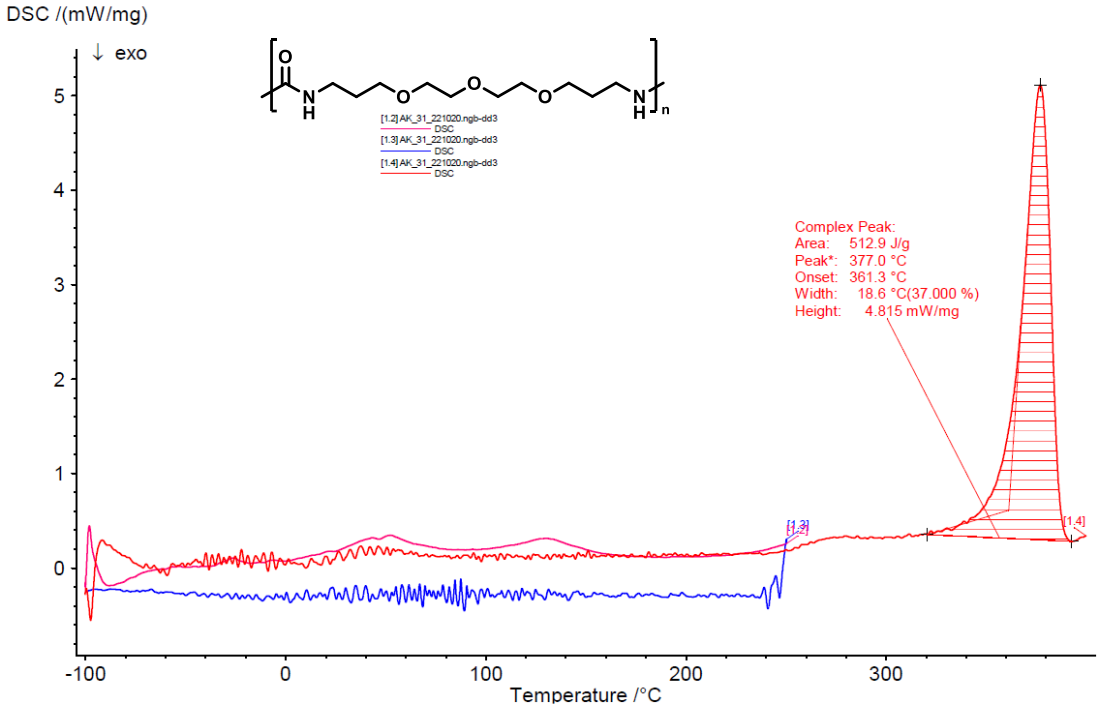

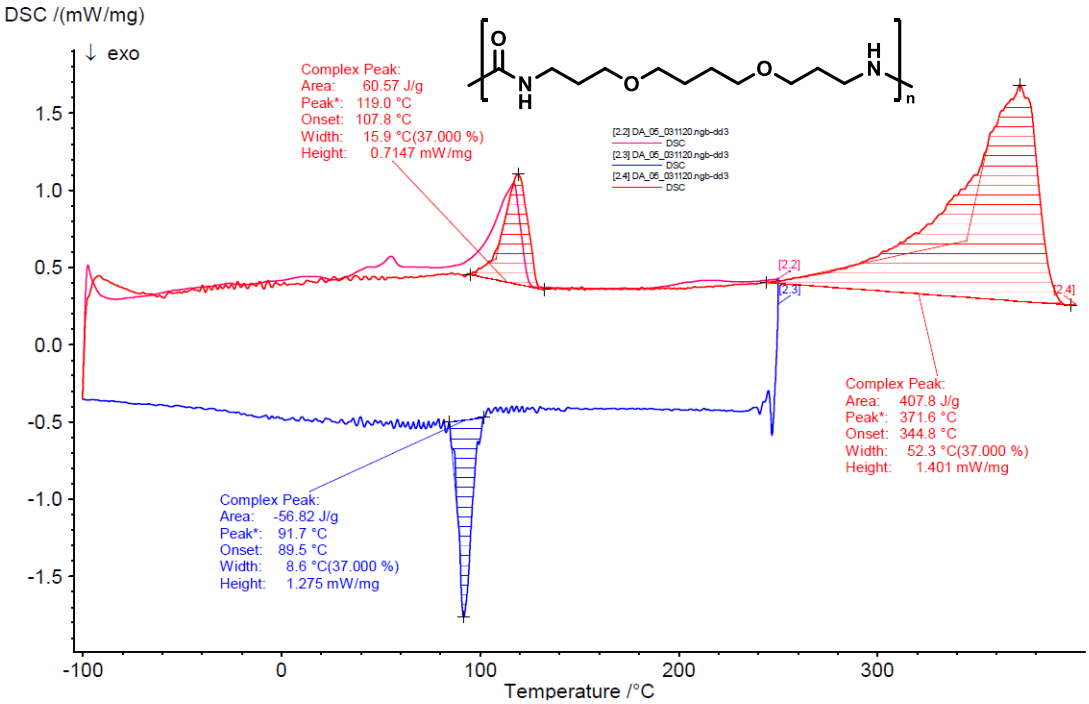

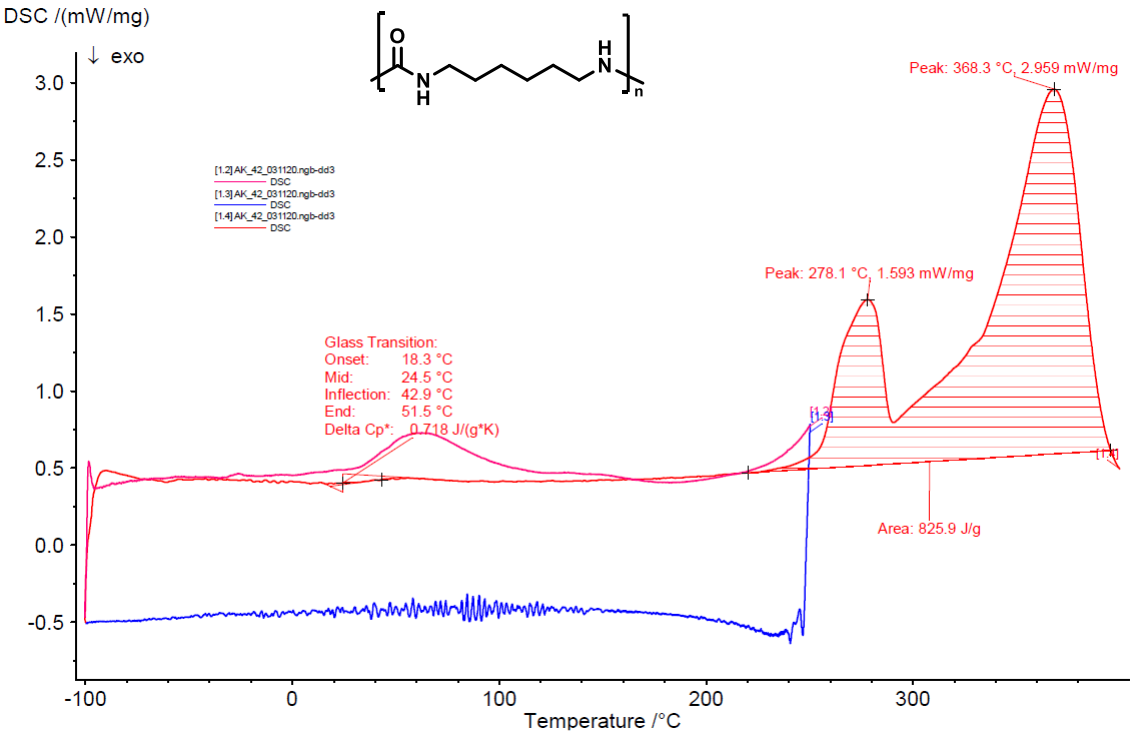
DSC /(mW/mg)
↓ exo
[1.2] AK_42_031120.ngb-dd3
DSC
[1.3] AK_42_031120.ngb-dd3
DSC
[1.4] AK_42_031120.ngb-dd3
DSC
Peak: 368.3 °C, 2.959 mW/mg
Peak: 278.1 °C, 1.593 mW/mg
Glass Transition:
Onset: 18.3 °C
Mid: 24.5 °C
Inflection: 42.9 °C
End: 51.5 °C
Delta Cp*: 0.718 J/(g*K)
[1.3]
[1.4]
Area: 825.9 J/g
3.0
2.5
2.0
1.5
1.0
0.5
0.0
-0.5
-100
0
100
200
300
Temperature /°C

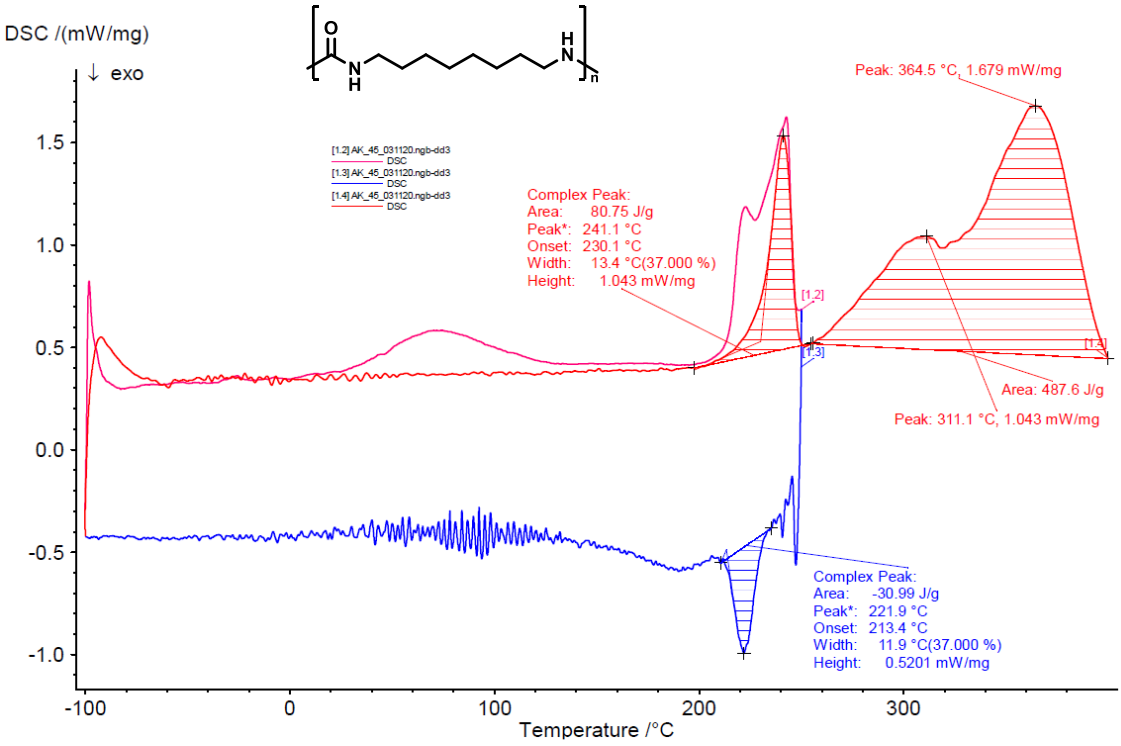
DSC /(mW/mg)
↓ exo
[1.2] AK_45_031120.ngb-dd3
DSC
[1.3] AK_45_031120.ngb-dd3
DSC
[1.4] AK_45_031120.ngb-dd3
DSC
Peak: 364.5 °C, 1.679 mW/mg
Complex Peak:
Area: 80.75 J/g
Peak*: 241.1 °C
Onset: 230.1 °C
Width: 13.4 °C(37.000 %)
Height: 1.043 mW/mg
[1.2]
[1.3]
[1.4]
Area: 487.6 J/g
Peak: 311.1 °C, 1.043 mW/mg
Complex Peak:
Area: -30.99 J/g
Peak*: 221.9 °C
Onset: 213.4 °C
Width: 11.9 °C(37.000 %)
Height: 0.5201 mW/mg
1.5
1.0
0.5
0.0
-0.5
-1.0
-100
0
100
200
300
Temperature /°C

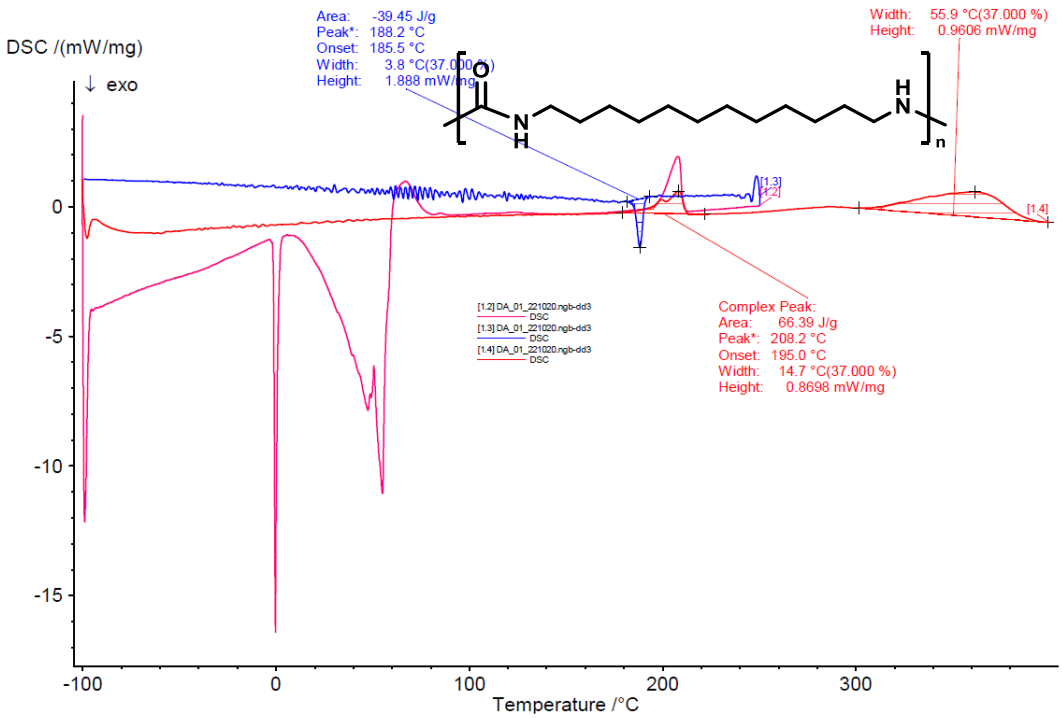
DSC /(mW/mg)
↓ exo
Area: -39.45 J/g
Peak*: 188.2 °C
Onset: 185.5 °C
Width: 3.8 °C(37.000 %)
Height: 1.888 mW/mg
Width: 55.9 °C(37.000 %)
Height: 0.9606 mW/mg
[1.3]
[1.2]
[1.4]
[1.2] DA_01_221020.ngb-dd3
DSC
[1.3] DA_01_221020.ngb-dd3
DSC
[1.4] DA_01_221020.ngb-dd3
DSC
Complex Peak:
Area: 66.39 J/g
Peak*: 208.2 °C
Onset: 195.0 °C
Width: 14.7 °C(37.000 %)
Height: 0.8698 mW/mg
0
-5
-10
-15
-100
0
100
200
300
Temperature /°C

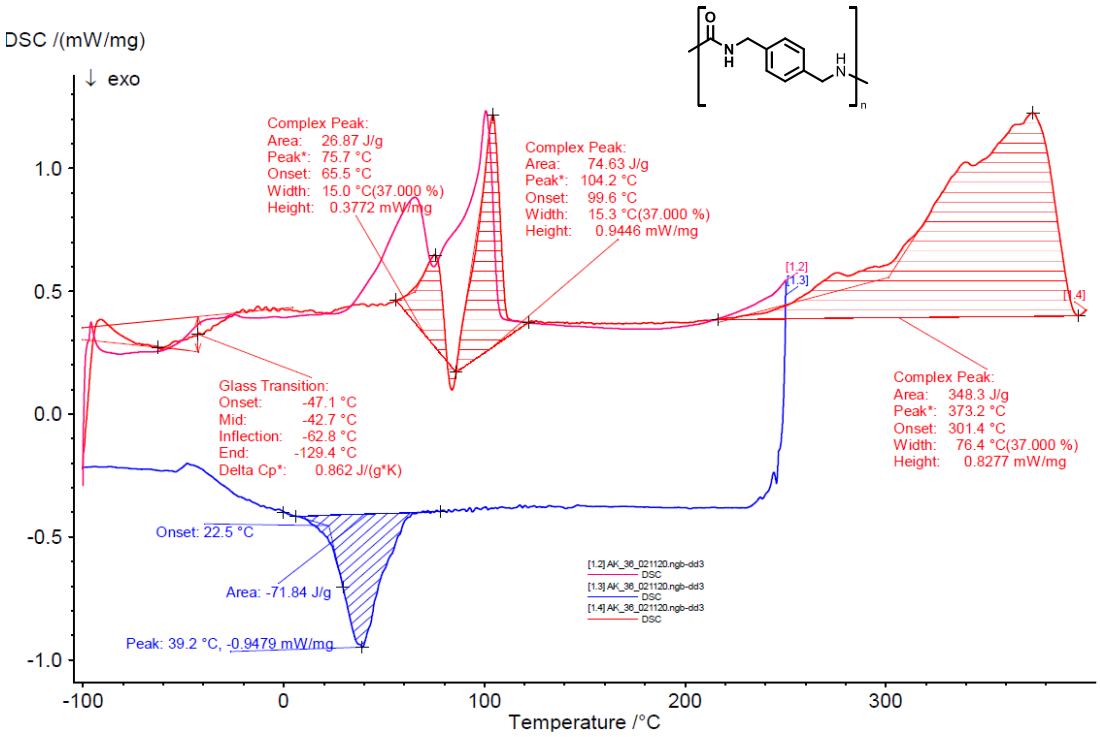
DSC /(mW/mg)
↓ exo
Complex Peak:
Area: 26.87 J/g
Peak*: 75.7 °C
Onset: 65.5 °C
Width: 15.0 °C(37.000 %)
Height: 0.3772 mW/mg
Complex Peak:
Area: 74.63 J/g
Peak*: 104.2 °C
Onset: 99.6 °C
Width: 15.3 °C(37.000 %)
Height: 0.9446 mW/mg
[1.2]
[1.3]
[1.4]
Glass Transition:
Onset: -47.1 °C
Mid: -42.7 °C
Inflection: -62.8 °C
End: -129.4 °C
Delta Cp*: 0.862 J/(g*K)
Complex Peak:
Area: 348.3 J/g
Peak*: 373.2 °C
Onset: 301.4 °C
Width: 76.4 °C(37.000 %)
Height: 0.8277 mW/mg
Onset: 22.5 °C
Area: -71.84 J/g
Peak: 39.2 °C, -0.9479 mW/mg
[1.2] AK_36_021120.ngb-dd3
DSC
[1.3] AK_36_021120.ngb-dd3
DSC
[1.4] AK_36_021120.ngb-dd3
DSC
1.0
0.5
0.0
-0.5
-1.0
-100
0
100
200
300
Temperature /°C

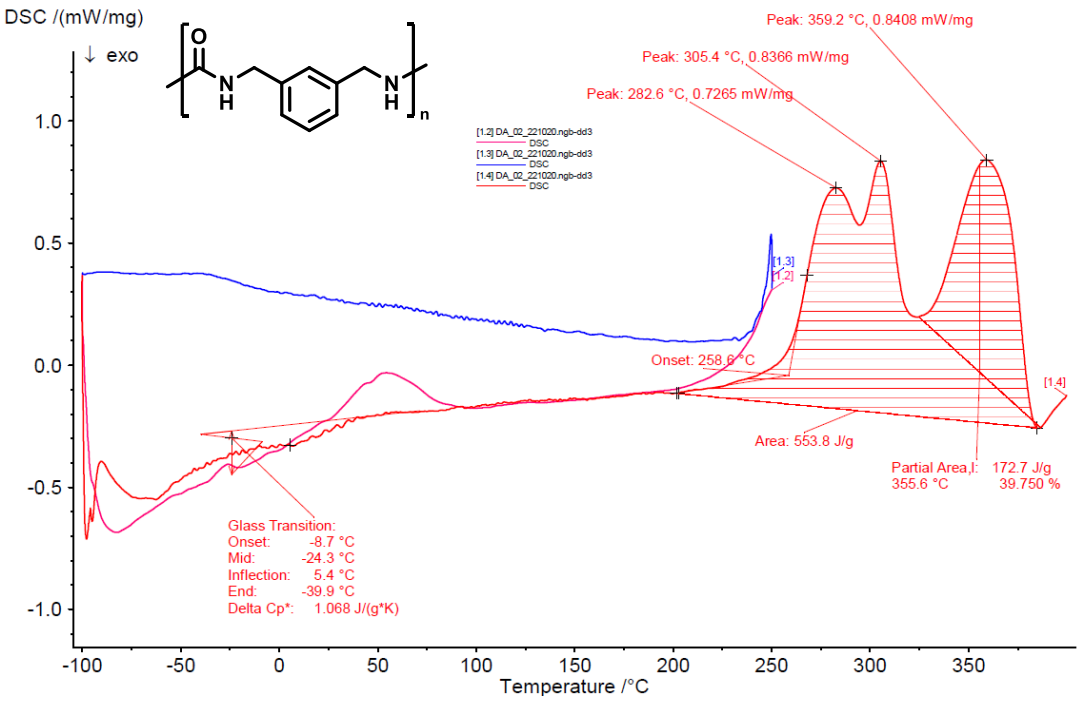
DSC /(mW/mg)
↓ exo
Peak: 359.2 °C, 0.8408 mW/mg
Peak: 305.4 °C, 0.8366 mW/mg
Peak: 282.6 °C, 0.7265 mW/mg
[1.2] DA_02_221020.ngb-dd3
DSC
[1.3] DA_02_221020.ngb-dd3
DSC
[1.4] DA_02_221020.ngb-dd3
DSC
[1,3]
[1,2]
Onset: 258.6 °C
[1,4]
Area: 553.8 J/g
Partial Area I: 172.7 J/g
355.6 °C 39.750 %
Glass Transition:
Onset: -8.7 °C
Mid: -24.3 °C
Inflection: 5.4 °C
End: -39.9 °C
Delta Cp*: 1.068 J/(g*K)
1.0
0.5
0.0
-0.5
-1.0
-100
-50
0
50
100
150
200
250
300
350
Temperature /°C

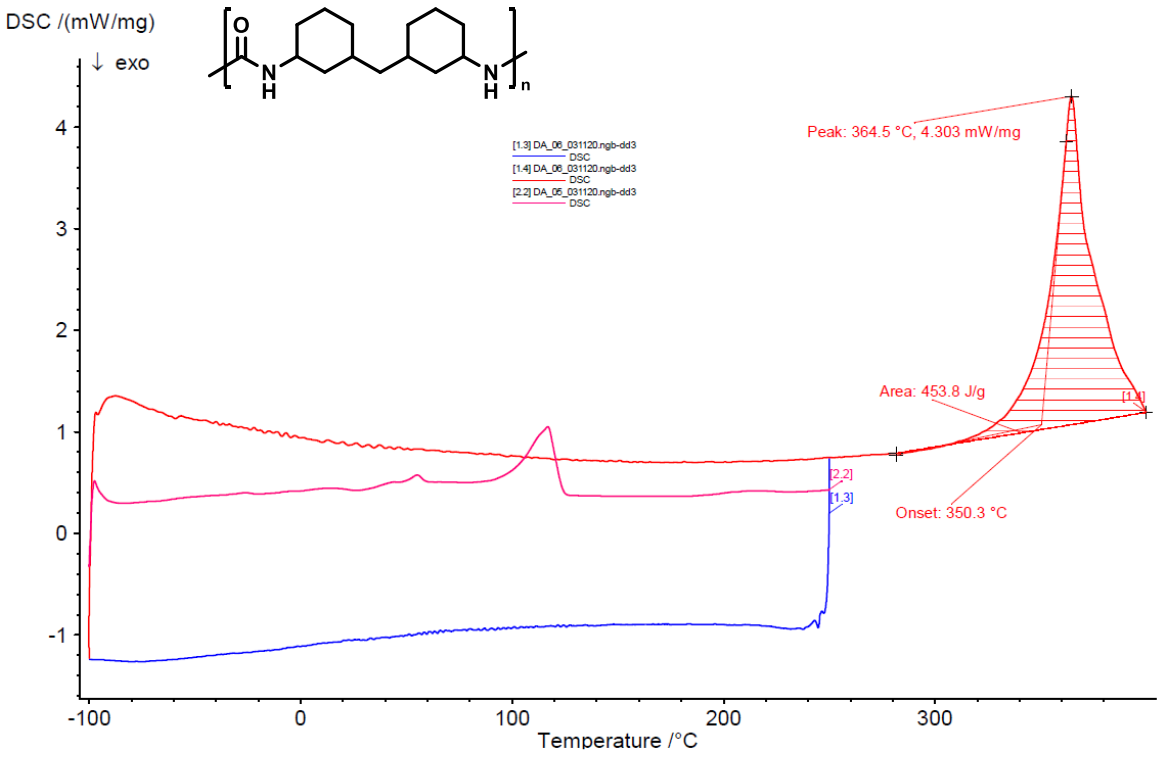
DSC /(mW/mg)
↓ exo
[1.3] DA_06_031120.ngb-dd3
DSC
[1.4] DA_06_031120.ngb-dd3
DSC
[2.2] DA_05_031120.ngb-dd3
DSC
Peak: 364.5 °C, 4.303 mW/mg
Area: 453.8 J/g
[1,4]
[2,2]
[1,3]
Onset: 350.3 °C
4
3
2
1
0
-1
-100
0
100
200
300
Temperature /°C

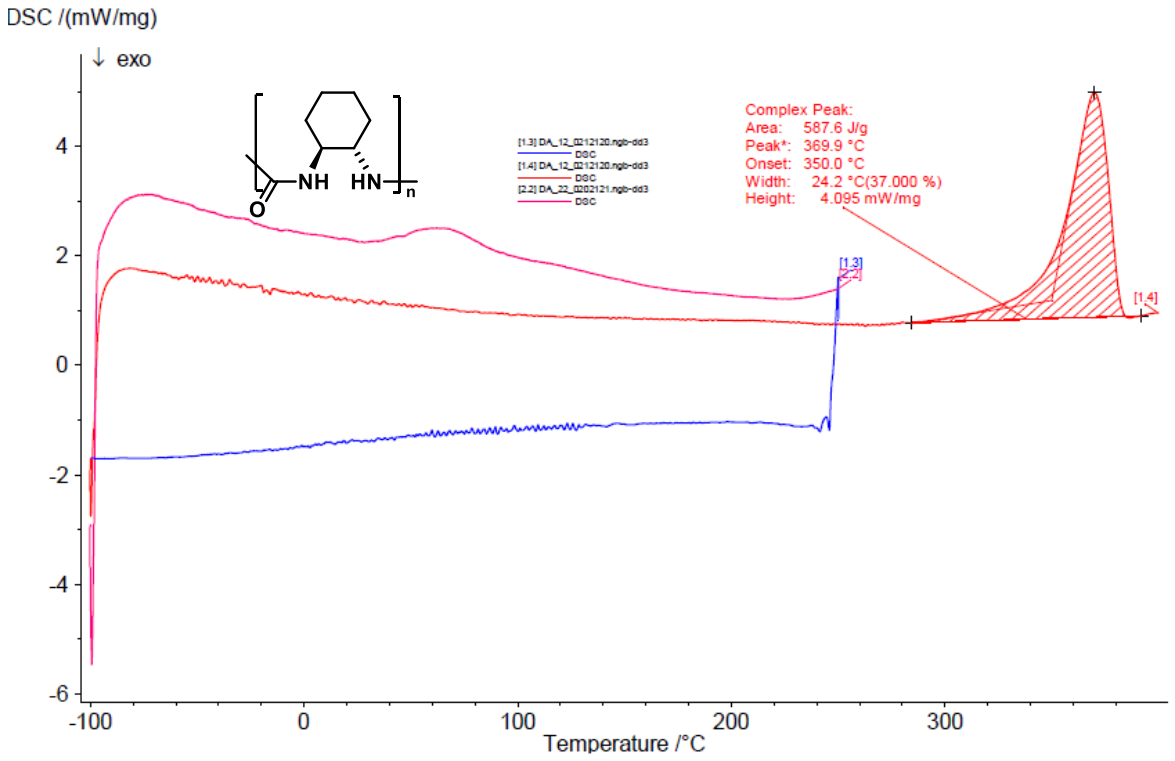
DSC /(mW/mg)
↓ exo
NH
HN
n
O
[1.3] DA_12_021220.ngb-dd3
DSC
[1.4] DA_12_021220.ngb-dd3
DSC
[2.2] DA_22_020221.ngb-dd3
DSC
Complex Peak:
Area: 587.6 J/g
Peak*: 369.9 °C
Onset: 350.0 °C
Width: 24.2 °C(37.000 %)
Height: 4.095 mW/mg
[1,3]
[2,2]
[1,4]
4
2
0
-2
-4
-6
-100
0
100
200
300
Temperature /°C

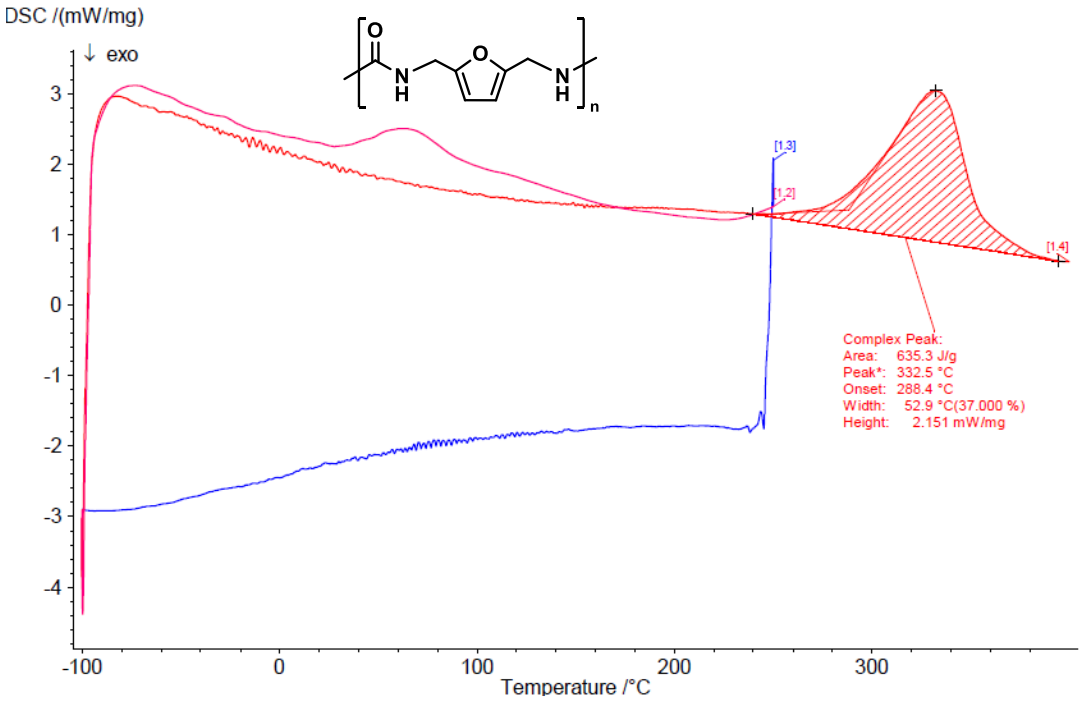
DSC /(mW/mg)
↓ exo
O
N
H
O
N
H
n
[1,3]
[1,2]
[1,4]
Complex Peak:
Area: 635.3 J/g
Peak*: 332.5 °C
Onset: 288.4 °C
Width: 52.9 °C(37.000 %)
Height: 2.151 mW/mg
3
2
1
0
-1
-2
-3
-4
-100
0
100
200
300
Temperature /°C

15. References

1. M. Nielsen, E. Alberico, W. Baumann, H. J. Drexler, H. Junge, S. Gladiali and M. Beller, *Nature*, 2013, **495**, 85–89.

2. N. Sieffert , R. Reocreux , P. Lorusso , D. J. Cole-Hamilton and M. Buehl , *Chem. – Eur. J.*, 2014, **20** , 4141-4155.

3. T. Yamanobe, I. Ando, H. Saito, R. Tabeta, A. Shoji, T. Ozaki, *Bull Chem. Soc. Jpn*, 1985, **58**, 23-29.

4. L. Moreno-Vilet, S. Bostyn, J.-L. Flores-Montaño and R.-M. Camacho-Ruiz, *Data Br.*, 2019, **24**, 103984.

5. B. Gnanaprakasam, E. Balaraman, C. Gunanathan and D. Milstein, *J. Polym. Sci. Part A Polym. Chem.*, 2012, **50**, 1755–1765.